Heterogeneity and Depositional Variability of Reef Sand Aprons: Integrated Field and Modeling of the Dynamics of Holocene Aranuka Atoll, Republic of Kiribati, Equatorial Pacific

By

Hannah Nicole Wasserman

Submitted to the graduate degree program in Geology and the Graduate Faculty of the University of Kansas in partial fulfillment of the requirements for the degree of Master of Science.

_____

Chair: Dr. Eugene Rankey

_____

Dr. Stephen Hasiotis

_____

Dr. Stacy Lynn Reeder

Date Defended: July 22, 2013

The Thesis Committee for Hannah Nicole Wasserman

certifies that this is the approved version of the following thesis:

Heterogeneity and Depositional Variability of Reef Sand Aprons: Integrated Field and Modeling of the Dynamics of Holocene Aranuka Atoll, Republic of Kiribati, Equatorial Pacific

_____

Chair: Dr. Eugene Rankey

_____

Dr. Stephen Hasiotis

_____

Dr. Stacy Lynn Reeder

Date approved:

**Abstract**

Depositional facies represent the net product of a complex set of processes that impact sediment supply and transport through geomorphic systems. Although the general facies motifs of many isolated platforms throughout the geologic record are well documented, the details of geomorphological and sedimentological patterns, and the physical oceanographical processes controlling sedimentological differentiation, are less well constrained. On isolated carbonate platforms, accumulation of reef-derived debris in platform-top reef sand aprons form expansive geomorphic elements, and can host prolific hydrocarbon reserves. To better understand the nature and scale of reef sand apron accumulations, this project integrates remote sensing, field, petrographical, and granulometrical observations of surficial Holocene sediments with physical oceanographical observations and modeling of Aranuka Atoll, Republic of Kiribati in the western equatorial Pacific.

These results illustrate trends in hydrodynamics, geomorphology, and sedimentology from the platform margin to the platform interior. Current meter data and modeling illustrate how the tides (2.5 m spring tidal amplitude) modulate wave energy (open-ocean, annual average swell height of ~2 m; distal swell height can be larger) to produce dominant on-platform flow (speeds up to 90 cm/s) on the northern reef sand apron. These hydrodynamical influences are interpreted to have led to the development of the expansive northern reef sand apron (>2000 m wide); the southeastern apron, with currents that reverse with the tides, includes a narrower sand apron. Concomitantly, the hydrodynamical patterns and platformward decrease in energy across the reef sand apron, coupled with changes in biota, are interpreted to control variability in sedimentary

structures, bottom types and sediment attributes. Sediment near the margin on the reef sand apron contains well-sorted coral and red algal-rich coarse sand and gravel, transitioning to poorly sorted, foraminifera-rich, medium to coarse sand toward the lagoon. The lagoon includes even finer sediment.

Collectively, the results of this study illustrate that selective winnowing, differentiation of sediment size, type, and sorting (e.g., depositional porosity and permeability), and nature and size of geomorphic elements, are linked ultimately to the hydrodynamical patterns across the platform. The results of this study provide a predictive conceptual model for the depositional variability and processes active on reef sand aprons, including some ancient reservoir analogs.

**Acknowledgements**

This study was funded through the Kansas Interdisciplinary Carbonate Consortium (KICC). First, I thank my advisor, Dr. Rankey, for all his time and support over the last two years. Because of him, I have grown as a researcher, and as a person. Also thanks to my committee members Dr. Hasiotis and Dr. Reeder for their time and effort during the writing process.

Thanks to the people of Kiribati and to the Kiribati Ministry of Fisheries and Marine Resources Development who granted the research permit. The Ministry was extremely helpful in providing personnel to aid in fieldwork and logistics. A special thanks to Tion Uriam for his time and hard work in the field; my research could not have been completed without him. Michelle Mary was also extremely helpful during fieldwork, but moreover she has been an invaluable friend and colleague. The Island Council of Aranuka was a wonderful host and also assisted in the project in numerous ways. Special thanks to Mayor Taiki of Aranuka for his guidance throughout the trip. Christian Appendini Albrechtsen provided vital assistance with MIKE21 modeling, and this modeling project could not have been completed without him. Thanks to Dr. Leigh Sterns for help with the Differential Global Positioning Satellite equipment, including training and post processing. Also, thank you to Katherine Liebetrau for her help during data analysis.

Finally, I thank my amazing family, especially my father, who has supported me through thick and thin. All of my achievements I attribute to them for raising me to be the best person I can be, and always pushing me to strive for success.

## Table of Contents

## List of Figures and Tables

FIGURES



TABLES

## Introduction

At a large geomorphic scale, carbonate systems have been classified as ramps, rimmed shelves, or isolated platforms (Wilson, 1975; Read, 1985; Handford and Loucks, 1993; cf. Williams et al. 2011). Isolated carbonate platforms, perhaps the iconic carbonate system, occur throughout the stratigraphic record, and commonly include considerable sedimentological variability (Stoddart, 1969; Wilson, 1975; James, 1983; Read, 1985; Pomar, 2001). One means to explore possible heterogeneity in ancient systems is by studying modern analogs. Modern carbonate systems provide the unique opportunity to explore the interrelations between processes and sedimentological products (i.e., sediment size, type, and sorting), and to explore the characteristics and scales of geomorphic belts and of sedimentological variability among and within environments.

In this context, many modern and ancient isolated carbonate platforms include lateral geomorphic changes, from reef to reef sand apron to lagoon. To understand controls on these patterns, Rankey and Garza-Perez (2012) compared widths of geomorphic elements (reef and reef sand apron) to such oceanographic parameters as sea-surface temperature, annual average significant wave height, and tidal amplitude on over 60 Holocene isolated carbonate platforms around the world. Results revealed that no one environmental parameter is the sole control of reef or reef sand apron width; instead, the reef sand apron width is a function of multiple environmental factors, including wave height and period, tidal amplitude, and margin orientation relative to wind and wave direction.

Similarly, on any one platform, such environmental factors as waves and tides control the energy level on reef sand aprons that, in turn, transport sediment (Weins, 1962; Stoddart, 1969; Gourlay, 1988; Kench, 1998a, 1998b, 1999c; Brander et al., 2004; Kench and Brander, 2006; Harris et al., 2011; Rankey et al., 2011). This sediment movement drives the progradation of sand aprons towards the lagoon (Marshall and Davies, 1982; Purdy and Gischler, 2005). Although numerous studies of Holocene and ancient isolated platforms describe a geomorphic pattern from general reef to reef sand apron to lagoon environments, few systematically describe the sedimentological variability. Still fewer capture the physical oceanographical processes controlling the sedimentological differentiation and facies transitions. To better understand the depositional variability and controls on reef sand apron accumulations, this study integrated remote sensing, field, petrographic, and granulometric observations of surficial Holocene sediments with hydrodynamical data and modeling from Aranuka Atoll of the equatorial Pacific.

**Background – Study Area**

Aranuka Atoll, located in the western equatorial Pacific, covers ~72 $km^2$ and is one of 32 atolls in the Republic of Kiribati. Aranuka Atoll is part of the Gilbert Island chain, which is comprised of five reef islands and eleven atolls (Fig. 1). Aranuka is triangular in shape and includes two large islands; one is oriented north–south on the eastern margin of the atoll and the other trends east–west on the western margin. Between the islands on the northern margin and much of the southern margin, an

intertidal to subtidal reef sand apron nearly 2 km wide extends from the margins inboard, toward the shallow (<18 m) lagoon (Fig 1). An annular reef with only one opening, on the southern margin, rims the atoll.

Aranuka Atoll is influenced by dominant easterly trade winds that generate persistent open-ocean waves, although during El Niño phases, winds are more variable and can come from the west (Richmond, 1993) (Fig. 2A–B). With the typical easterly trade winds, the dominant wind component shifts from northeasterly during the months of January through June to southeasterly from July to December (Richmond, 1993). Locally generated open-ocean wind waves vary seasonally, and can propagate from either the northeast or southeast (Barstow and Haug, 1994), according to the wind direction (Fig. 2C–D). Open ocean swell is also variable. Waves can propagate from the southwest (from the south Pacific and Southern oceans) as well as from the northwest, and caused by northern hemisphere cold fronts from October to March (Barstow and Haug, 1994). The annual average open-ocean swell height in the area is ~2 m (Richmond, 1993). The open-ocean swell breaks on the reef margin or the islands, but smaller wind-generated waves occur in the platform interior. Other than wave forcing, semidiurnal tides also influence the hydrodynamics of the platform; spring tidal amplitude is > 2.5 m.

Due to the equatorial location, Aranuka Atoll is not directly influenced by tropical cyclones (Sachet, 1957; Rankey, 2011), and processes unrelated to tropical depressions have the largest impact on platform hydrodynamics (Rankey, 2011; cf. Scoffin and Tudhope, 1988; Tudhope, 1989). The climate of Aranuka is tropical, with the annual air temperature in the Gilberts ranging from 28–30$^{\circ}$ C and an average water temperature of 27$^{\circ}$ C (Richmond, 1993). Upwelling also influences this equatorial Pacific region, by

bringing cool, nutrient-rich waters to the surface (Wyrtki and Eldyn, 1982; Chavez et al., 1999).

**Methods**

QuickBird remote sensing data revealed a diversity of geomorphic elements across the platform including reef, reef sand apron, lagoon, patch reefs, and islands. Remote sensing data analysis prior to fieldwork provided a spatial context for data collection and analysis.

To capture the range of variability in sedimentology and bottom types within and among geomorphic elements, 236 surface sediment samples were collected from 12 transects across the atoll with a sampling interval of 100 m. Samples were collected using small plastic vials (44, 74, or 148 ml) and capped at depth to preserve any fines. A qualitative estimation and description of the sedimentological and ecological aspects at each location—abundance of benthic organisms; presence, visual estimation of abundance, and type of burrowing organisms; and physical sedimentary structures—recorded for each field collection site provide bottom type information and context for samples. The location of each observation point was marked with a hand-held GPS. Bottom type at each sample location on the reef sand apron was quantitatively described in 50 m intervals using a 25 m margin parallel transect (similar to the methods of Frank and Jell, 2006).

Following the collection of sediment samples, laboratory analyses quantified grain type and size. GRADISTAT software (Blott and Pye, 2001) calculated particle size statistics for each sample, including mean grain size and sorting using the Folk and Ward

(1957) classification where lower ϕ values indicated better sediment sorting. Thin sections (N=92) of unsorted sediment captured the range of variability in sedimentology and bottom type from within and among geomorphic elements across the atoll, similar to the methods of Rankey et al. (2011). Abundance of grain types was estimated semiquantitatively from thin sections under a petrographic microscope, following the methods of Rankey and Reeder (2010). A large proportion of the sediment (average 53% among thin sections) was characterized as petrographically unidentifiable skeletal fragments, because thin sections were made using unsorted samples, and because many grains were highly abraded, bored, or encrusted. All field observations and laboratory measurements were integrated with ArcGIS to more easily evaluate geomorphological and sedimentological trends across the reef sand aprons.

To further understand the hydrodynamics of the atoll, a bottom-mounted SonTek current meter measured waves and currents for 9 weeks (August 15–October 17, 2012), across several tidal cycles, within a channel on the northern reef sand apron (Fig. 1). Daily exposure of much of the intertidal sand apron combined with a desire for continuous data collection and a requirement for the meter to be submerged to protect the instrument, mandated deployment of the *in situ* current meter in a channel that remained submerged at spring low tide. Waves and currents were measured at 4 Hz with a burst duration of 1024 seconds and a burst interval of 1200 seconds.

The measured data, from one point through time, are not representative of the entire atoll. These field data, therefore, were supplemented with MIKE 21 hydrodynamic (HD), a hydrodynamical mapping and modeling program, to model 2 dimensional (2D) hydrodynamics across Aranuka Atoll. Moreover, this modeling program provides a

means to systematically explore and access the influence of individual controls including winds, waves, and tides, on the spatial variability in current patterns across the atoll. MIKE 21 HD is the basic module of the MIKE 21 system and simulates water level variations, as well as current speed and direction, using model responses to several factors (DHI Water and Environment, 2007). These factors include bottom shear stress, wind shear stress, wave radiation stress, flooding and drying, barometric pressure gradient, momentum dispersion, evaporation, and sources and sinks (DHI Water and Environment, 2007).

Three MIKE 21 HD simulations of the atoll included: 1) a wind-only simulation, using winds from the east ($90^{\circ}$) at 10 m/s, which generates local wind waves; 2) a tides-only simulation, with tides of 2.5 m amplitude; and 3) a distal waves-only simulation, using waves ($H_s$ = 2 m and 4 m) generated from the north ($0^{\circ}$) to mimic swell from distant northern hemisphere cold fronts (for details on each model, see Table 1). External model components included a generalized bathymetric grid (50 $m^2$ cell size) and NOAA tide data (http://tidesandcurrents.noaa.gov) applied as boundary conditions. The MIKE21 Nearshore Spectral Waves (NSW) module created a wave radiation stresses file that was fed into the MIKE21 HD model to simulate the waves. The details of model specific setup are described below (Table 1). The purpose of these models was to characterize the first order patterns in flow velocity from wind, wave, and tidal forcing to aid conceptual understanding, rather than to reproduce the details and complexities of the actual current patterns on the atoll for any specific time period. Bearing in mind the limited data available for Aranuka Atoll, each model was simplified by varying only the wind, wave, and tidal parameters. By holding all other parameters constant among simulations, this

allows for a better evaluation and interpretation of the modeling results from each forcing agent.

## Results

*Geomorphology and Sedimentology*

Aranuka Atoll contains a range of geomorphic elements, including forereef, reef crest, reef sand apron, lagoon (including patch reefs), and island (Fig. 1). The upper forereef, seaward of the reef crest, includes well-developed spurs and grooves (e.g., Munk and Sargent, 1954; Wiens, 1962; Shinn, 1963). The margin-normal spurs and grooves may extend up to 300 m from the reef crest towards the open ocean, and are present around most of the atoll (Fig. 3). The spur and groove system extends from water depths of several meters near the reef crest to 10's of meters toward the open ocean. The spurs are covered predominantly by a coral and algal framework growth and stand up to ~3 m above intervening grooves. Between the spurs are the lows of the grooves, which range from < 1 m to a few 10's of meters wide, and which include a range of grain sizes, from coral-algal boulders and rubble to sand.

Bathymetrically above and platformward of the spur and groove system, a pavement of encrusting coralline red algae forms the reef crest (James, 1983; comparable to the coral algal ridge of Odum and Odum, 1955, algal ridge of Weins, 1962, or reef rim of Woodroffe and Biribo, 2011) around most of the atoll (Fig. 3). This reef crest remains submerged and washed with waves, except during spring low tide or other exceptional periods. Sediment on the reef crest consists of reef detritus (e.g., fragments of coralline red algae, corals, and foraminifera), but is generally thin and patchily distributed. The

reef crest reaches up to 60 m across and gradationally transitions platformward into the reef sand apron, which lies topographically lower (< 1 m) than the reef crest.

The most extensive geomorphic constructs of Aranuka Atoll, and the focus of this study, are the northern and southern reef sand aprons (Fig. 1). These intertidal to subtidal features dip gently (<0.1°, but see detailed discussion below) and extend up to 2 km before passing into the lagoon as sediment constituents vary. The sediment of this region includes red algae (average 16%), benthic foraminifera (average 15%), coral fragments (average 6%), and bivalve fragments (average 6%), as well as minor enchinoderm spines, gastropods, *Halimeda,* and bryozoans.

On these sand aprons, remote sensing data calibrated by field observations of the bottom type illustrate three margin-parallel subzones (Fig. 3): 1) an amalgamated- to closely spaced-microatoll subzone; 2) an aligned coral subzone; and 3) a mobile sand subzone. Within ~300 m of the reef crest, the reef sand apron includes an amalgamated- to closely spaced-microatoll subzone comprised of *Heliopora* and *Porites* microatolls (Fig. 4A). This subzone remains submerged at low tide. Between the corals and microatolls, in lows <50–75 cm below the crest of the microatolls, a dominantly rocky bottom includes only thin (<5 cm), patchy accumulations of sediment. Sediment within this subzone consists of very well-sorted (sorting = 1.21 $\phi$), red algal-rich, coarse sand and gravel (mean grain size of 1286 μm; N=15) (Fig. 5).

At distances > 300 m platformward of the reef crest, the closely spaced coral cover transitions gradually into the aligned coral ridge subzone (Woodroffe and Biribo, 2011), which includes margin-normal ridges and coral-poor, rocky to sediment-covered lows. The ridges (up to ~20 m wide, narrowing platformward) include amalgamated

microatolls and isolated corals that stand ~30–60 cm higher than intervening rocky to sand and rubble filled lows that generally broaden platformward and can reach up to ~60 m wide (Fig. 4B). On the remote sensing data and low angle aerial photos (Fig. 3), the coral-rich ridges form a distinct, pin-stripe pattern that extends up to 400 m towards the platform interior. Similar to the amalgamated- to closely spaced-microatoll subzone, observations from the field reveal that the aligned coral ridge subzone is completely submerged, even at spring low tide. The ridges themselves are coral rich, similar to the amalgamated- to closely spaced-microatoll subzone (Fig. 4A). Sediment within the aligned coral subzone consists of moderately sorted (sorting = 1.64 $\phi$), coarse sand to gravel (mean grain size of 998 μm; N=27) (Fig. 5).

At distances > ~700 m from the platform margin, across several 10s to 100s of meters, the coral-rich ridges of the aligned coral subzone transition into, and interfinger with, the sediment of the mobile sand subzone (similar to the zone of sand and shingle described by Odum and Odum, 1955*)*. This subzone is the platformmost portion of the reef sand apron, and includes the most pronounced relief present on the sand apron. The mobile sand subzone on the northern apron ranges from broad, shallow (<3 m deep at low tide) subtidal to intertidal channels flanked by margin-normal supratidal sand and gravel barforms. The barforms are elongate (up to 1.2 km long and 80 m wide) in the direction of predominant, on-platform flow, but they are typically asymmetric in cross section, with a steeper margin to the west. These margin-normal bars are present platformward of earlier Holocene rocky islands and form the flanks of the subtle (<3 m deep) subtidal to intertidal channels (Fig. 6). Margin-normal bars and channels are poorly developed on the southern margin.

The intertidal to supratidal barforms of the mobile sand subzone typically occur in the lee of earlier Holocene (rocky) islands and include up to 80 cm of local relief, with superimposed dunes (6–14 cm high) and current ripples (1–3 cm high), both of which are flood oriented, on their crests and flanks (Fig. 6C). The sedimentology of the barforms is spatially variable. On the northern sand apron, the sedimentology of the barforms gradationally transitions platformward over ~600 m (Fig. 6A). The gravel-dominated barforms are present within the first 300–400 m (1.1 km from margin) of the mobile sand subzone and include well-sorted, very coarse sand and gravel on bar crests (mean grain size is 1269 μm and sorting is 0.255 ϕ, very well-sorted; N=1). Off the crest of the gravel bars, sediment is finer (mean grain size is coarse sand, 808 μm; N=4, with grain size that ranges from medium to coarse sand; 465–979 μm) and less well sorted (mean sorting is 0.89 ϕ, moderately sorted, but sorting ranges from 0.69-1.30 ϕ). Further inboard, barform crests gradationally transition into sand. For example, sediment on the bar crests >1.1 km inboard from the margin consists of coarse to very coarse sand (mean grain size is 900 μm, but grain size ranges from 575–1355 μm N=13) and is moderately sorted (mean sorting = 0.82 ϕ, but ranges from 0.24–1.3 ϕ). Off the crest of the bars here, sediment is finer (mean grain size = 583 μm, but ranges from medium to coarse sand; 463–1016 μm N=22) and more poorly sorted (sorting = 1.1 ϕ, but ranges from 0.79–1.3 ϕ) than on the bar crest.

Channels that cross the mobile sand subzone are all <3 m deep at low tide. Individual channels that start as broad, subtle (cms of relief) depressions up to 1 km wide near the margin pass into narrower and deeper channels towards the lagoon. In cross section, the largest channel on the northern reef sand apron has a steeper gradient (near

angle of repose) on the eastern margin, compared to a gentler gradient (0.07°) on the western flank. Within channels, small amplitude, flood-oriented subaqueous dunes (up to ~20 cm high and up to ~150 cm spacing) can include superimposed ripples (up to ~7 cm high and up to ~15 cm spacing). Sediment in the deeper (>2 m) portion of channels consists of moderately sorted, coarse sand (mean grain size 818 μm and sorting = 0.90 ϕ; N = 5); the shallower flanks of channels include finer and more poorly sorted sediment (mean grain size 677 μm, coarse sand and sorting = 1.17 ϕ; N = 16). In all, sediment within the subtidal channels has grain sizes broadly comparable to the surrounding intertidal sand apron (mean grain size of 711 μm, coarse sand; N= 21).

Many subtidal lows on the sand apron include a sandy bottom with up to ~150 burrows/$m^2$. Burrow openings reach up to 2 cm in diameter, whereas mounds can be up to ~9 cm in diameter at the base and 1–2 cm high (Fig. 4C). These burrowed areas also commonly include patchy, semicohesive orange diatomaceous mats as well as orange fleshy algae. Topographically higher (intertidal) areas on the mobile sand subzone include two-dimensional and three-dimensional, straight to sinuous crested to lingoid ripples (Fig. 4D); current ripples dominate. Collectively, sediment in the mobile sand subzone includes poorly sorted (sorting = 2.15 ϕ), foraminifera-rich, medium to coarse sand (mean grain size 658 μm; N=104).

In summary, the three subzones of the reef sand apron include systematic spatial patterns in bottom type, from coral rich and rocky near the margin to burrowed and rippled sand near the lagoon (Fig. 7). Similarly, trends in grain type, size, and sorting are evident within and among subzones. At the largest scale, red algal rich (in some locations >20%), very well-sorted, very coarse sand near the margin transitions

platformward into a foraminifera-rich (in some locations >50%), poorly sorted, medium to coarse sand near the lagoon (Figs. 8–9, Table 2).

In many locations, the northern and southern reef sand aprons gradationally transition (<0.1°) to the lagoon, such as south of the margin-parallel bar on the northern reef sand apron, and east of the reef opening on the southeastern reef sand apron. There are locations, however, where there is a more pronounced drop from the reef sand apron into the lagoon such as east of channel on the northern reef sand apron (1.4° over ~200 m; Fig. 7B), west of the reef break on the southern apron (2.1° over 175 m), and near the platformmost edge of the largest channel on the northern sand apron (2.3° over ~330 m). The reef sand aprons pass laterally into the lagoon, except for locations where the apron intersects islands. The lagoon, which reaches depths of 18 m, consists of sandy to silty bottom with scattered seagrass and patch reefs. Many areas are bioturbated (>10 burrows and mounds/$m^2$); mounds are up to 20 cm in diameter at their base and range from 5–20 cm in height. Within the lagoon are isolated corals and patch reefs that are composed of *in situ* coral framework and vary in size from several small coral heads a few meters wide, to large pinnacles 100's of meters across, that can stand up to 10 m above the surrounding lagoon. Sediment within the lagoon was not studied in detail.

*Hydrodynamics – Observations*

Current meter data collected within a channel on the northern reef sand apron indicate the influence of both tides and waves on the hydrodynamics of the northern reef sand apron on Aranuka. During the collection period, currents were variable, and illustrate several first-order trends in current velocity. Current meter data demonstrate a

dominance of on-platform flow with speeds up to ~90 cm/s (Figs. 10–12). Data also illustrate a peak velocity change between spring and neap tides, with peak velocities reaching up to 60 cm/s during spring tide in contrast to ~20 cm/s during neap tide (Fig 10A). Over the data collection period, the current velocities >30 cm/s consistently have a current direction between 120°–140° (toward the southeast; on-platform). Although results illustrate a dominance of on-platform currents, the infrequent off-platform currents have lower velocities than on-platform currents. Within each semidiurnal tidal cycle, current speeds are greatest during early flood tide (Fig. 11A).

Over this same time frame, wave height, period, and direction varied; significant wave height ($H_s$) ranged from 0 cm to 26 cm and wave period ($T_s$) ranged from 0.5 sec to 20 sec. Data reveal that >60% of the waves during the collection period are propagating from the east (between 45° and 135°). The average wave direction was from the east-southeast (118°). Wave direction is correlated with the wind direction, which over the data collection period was dominantly from the east.

The currents do not reflect only tidal forcing, however. For example, the *in situ* current meter data captured a period of sustained, elevated on-platform currents that did not correspond with spring high tide. The event occurred over three days (October 11–13, 2012) and produced current velocities as high as ~90 cm/s—the highest recorded velocity over the 9 week data collection period (Fig. 12A). Current direction during this period ranged from 120°–180° (south-southeast, on-platform; Fig. 12B). Wave data collected during this event illustrate that waves at the location of the current meter were small (<10 cm) and with broadly similar direction to those of the rest of the data (Fig. 12C),

suggesting that this time was not anomalous in terms of local wind-generated wave activity.

*Hydrodynamics – Modeling*

Winds, tides, and waves can influence the hydrodynamics of platform systems. Modeling results reveal the influence of each variable. For example, current patterns from the simulation of easterly winds are dominated by unidirectional current across the atoll in the general direction of the wind movement (Fig. 13A); some flow is diverted around islands and several eddies develop (e.g., near the reef break on the southern margin and the west side of the main channel on the northern reef sand apron). High current speeds (up to ~50 cm/s) occur near the topographically high margins of the atoll, but decrease towards the lagoon, where speeds are generally <10 cm/s.

The tide simulation model illustrated different patterns. Specifically, current patterns from the tide model included currents that were stronger than the wind model and that changed direction (Figs. 13B–C). In both flood and ebb phases of the simulations, the strongest currents occur near the margin and decrease towards the lagoon (which includes currents up to ~55 cm/s) (Figs. 13B–C). The highest simulated velocity, ~110 cm/s, occurred in the reef break on the southern margin.

The distal wave model was initialized with waves from the north. The model generated currents in a generally southward direction, largely coincident with the wave propagation direction (Figs. 13D–E). This produces unidirectional current across the northern reef sand apron. Similar to both the wind and tide simulations, the wave model demonstrates higher current speeds up to 60 cm/s near the reef margin, and lower current

speeds (< 10 cm/s) in the bathymetrically deeper lagoon (Figs. 13D–E). Such locations as the channel on the northern reef sand apron and between margin-normal barforms on the northern reef sand apron show current speeds that are elevated relative to the surrounding apron (up to ~40 cm/s, compared with <20 cm/s).

## Discussion

### *Hydrodynamics – Interpretations*

The *in situ* current meter data (Figs. 10–12) from the northern reef sand apron illustrate a clear spring-neap pattern (Fig. 10), with peak velocities occurring during spring tides. Within each semidiurnal tidal cycle, the patterns change as well. Specifically, the highest on-platform current speeds of each tidal cycle occur during the early stages of the rising tide. This observation of elevated flood velocities is interpreted to reflect the interactions of the >2 m tidal range with subtle topographic variations on the reef sand apron. As the tide rises, much of the intertidal to supratidal sand apron is exposed; only the subtidal channels (e.g., the location of the current meter) that lie bathymetrically lower than the surrounding reef sand apron are flooded. In this situation, on-platform current during early rising tide is focused in bathymetric lows until water level rises sufficiently to overflow the channel and flood the surrounding intertidal to supratidal reef sand apron. At this point, the sand apron gradually submerges, current changes from confined to unconfined, and current velocities decrease markedly.

The pattern is not simply reversed during ebb tide, as would be expected in a purely tidal system (e.g., Fig. 13B). Instead, even during the falling (ebb) stage of the tidal cycle, the dominant current in this location is on-platform, suggesting the influence of another factor. Several possible factors could drive this on-platform flow, including

swells or wind-generated currents and waves. If wind-generated currents or local waves were directly influencing this on-platform flow, winds would have needed to be from the north, creating unidirectional flow from north to south across the reef sand apron (cf. Fig. 13A). This pattern, however, is inconsistent with the dominant easterly wind direction and the *in situ* observations of wave data collected by the current meter. These data illustrate low amplitude (average $H_s$ is 7.5 cm), low period (average $T_s$ is 1.8 sec) waves dominantly from the east, consistent with those waves being generated by the easterly winds, not northerly. Local wind-generated currents or waves are, therefore, not likely causing this dominant on-platform flow.

Another variable that could have a direct influence on this dominant on-platform current is distal swell, low-period waves generated outside of the area. The influence of distal swell is suggested by an event recorded during the data collection period. The Global WAVEWATCHIII archive (Fig. 14) illustrates the passage of a strong early winter cold front in the northwest Pacific on October 11–13, 2012. During this 3–day interval, unusually large waves (for the period for which current meter data were collected) propagated across the Pacific, and possibly impacted the Gilbert Island chain. On Aranuka, these large waves are interpreted to have broken at the margin (and hence are not evident as waves at the instrument location) and drove sustained, elevated south-southeasterly on-platform currents (~90 cm/s) from the margin over the reef sand apron (Fig. 12). A model that captures similar swell (Figs. 13D–E) illustrates how small (2 m or 4 m) distal swell can generate dominant unidirectional on-platform current across the atoll, comparable to the observations of the *in situ* current meter.

These observations and interpretations are consistent with other anecdotal evidence. Even though *in situ* current meter data recorded dominant on-platform current on the northern reef sand apron, this observation does not mean that currents of other locations around the atoll are always on-platform as well. Indeed, a number of locals living near the southeast margin of Aranuka Atoll indicated that rising tide is characterized by on-platform current, but that falling tide includes off-platform current. This bi-directional current suggests that the water flooding onto the platform from the northern margin exits the platform on the southern margin, including the reef channel (see Figs. 13B–E).

To summarize, the dominant on-platform current on the northern reef sand apron is most likely due to the coupled influence of tides and open-ocean swell. Due to the current reversing with the tides on the southern margin, it is probable that the southern margin reflects a stronger tidal influence than the northern margin. As a result, in this tide-dominated, wave-influenced system, hydrodynamical patterns and the influences of waves and tides vary spatially around the atoll. These hydrodynamical patterns might be expected to have an influence on the scale of geomorphic belts and of sedimentological variability among and within environments.

*Geomorphic and Sedimentological Patterns – Interpretations*

Numerous studies highlight hydrodynamical influences on geomorphology and sedimentological patterns (Purdy, 1963; Hine, 1977; Hine and Neumann, 1977; Rankey et al., 2009; Reeder and Rankey, 2009; Rankey and Reeder, 2010), most notably in such high-energy environments as reef, reef sand apron, or ooid shoal systems (Kench, 1998c;

Rankey and Reeder, 2011; Rankey et al., 2011). On Aranuka Atoll, observations reveal dominant on-platform current on the northern margin. The dominant on-platform current here would favor unidirectional sediment transport across the reef sand apron and towards the lagoon. The broad northern reef sand apron on Aranuka, which at >2 km is one of the widest in the world, was most likely caused by the dominant on-platform current in the north. This same on-platform current pattern is not present on the southeastern margin. Instead, the narrower southeastern apron may reflect the more bidirectional flow in those areas, and include more off-platform transport.

Like the geomorphic patterns, the sedimentology (grain size, sorting, and type) along and across the reef sand apron is variable. Granulometric results (Figs. 8–9) show sediment near the margin on the reef sand apron is very well-sorted, very coarse sand and gravel, but that the sediment transitions platformward into poorly sorted, medium to coarse sand. Several studies (Wiens, 1962; Maxwell et al., 1964; Wilson, 1975; Montaggioni, 2005; Rankey et al., 2011) found broadly similar patterns in sediment size and sorting on Pacific reefs and atolls. Two end-member reasons may explain this sedimentological differentiation: 1) physical processes (hydrodynamics) that drive differential transport or winnowing; or 2) *in situ* production that generates sediment of different sizes at different points across the reef sand apron.

Hydrodynamical results from Aranuka Atoll indicate clear trends in velocity around the platform, with maximum current velocities near the margin that decrease towards the platform interior (Fig. 13). As such, one possible explanation of why sediments fine and are less sorted towards the platform interior is that they reflect variations in hydrodynamical energy, changes that drive differential winnowing along

flow paths. Sediment winnowing is controlled by the intensity of the hydrodynamics, with high-energy environments more effective at winnowing fine material than low-energy environments (Folk, 1962). On Aranuka, near the margin, the intense waves, tides, and currents winnow fines, which are then transported towards the platform interior (i.e., lagoon), where they can be sequestered due to insufficient energy for transporting sediment (Dunham, 1962; Rankey et al., 2011). In this context, if all sediment were reef derived, these hydrodynamics—higher energy near the margin, decreasing towards the lagoon—would produce coarser, better sorted sediment accumulations near the margin, fining and decreasing in sorting with increased distance from the source (e.g., towards the platform interior), consistent with the sedimentological patterns present on Aranuka.

Although the general patterns are consistent with differential transport, these same transport processes modify and breakdown the sediment, and may represent an additional influence on granulometric trends. During transport, such physical mechanisms as abrasion and chipping generate finer sediment (Maiklem, 1968). The finer sediment, is then more likely to be transported platformward via winnowing, re-enforcing the hydrodynamical processes that influence the sedimentological trends in grain size and sorting.

Although hydrodynamics appear to play an important role in the granulometric trends, another possible influence on the granulometric and grain type trends is *in situ* production. In carbonate systems, sediment can be produced at, and transported from, more than one location (e.g., the reef and reef sand apron). Multiple locations of *in situ* production within any environment (e.g., reef sand apron) can add nonreef-derived material, directly impacting the grain type, size, and sorting by adding sediment that is

not in equilibrium with the hydrodynamic conditions. Indeed, several studies have shown that *in situ* production is variable along a reef flat or reef sand apron environment (Yamano et al., 2000; Harney and Fletcher, 2003; Hart and Kench, 2007; Fujita et al., 2009). On Aranuka, organisms that may produce sediment *in situ* along a flow path include corals *(Heliopora* and *Porites)*, bivalves, and benthic foraminifera.

The Aranuka data (Fig. 9) reveal red algal-rich sediment (>30% in some locations) in areas with abundant coralagal growth (cf. Fig. 7) near the margin, and a transition into foraminifera-rich (>50% in some locations), bare sand in areas towards the platform interior. Although it is likely that *in situ* production is present across the reef sand aprons, if *in situ* production dominated in these geomorphic elements, the systematic change in grain attributes observed would not be expected due to the patchy addition of new sediment of various sizes across the reef sand aprons. Thus, although hydrodynamics are interpreted to be an important factor in the granulometric and grain type trends, sediment clearly can be created *in situ* and may account for some variability in sedimentological patterns.

Similarly, the change from coralgal to foraminifera-dominated sediment on Aranuka may be related to trends in the durability of different carbonate grains. Skeletal carbonate grains have variable durability, controlled by skeletal structure and mineral density (Sorby, 1879; Chave, 1964; Ford and Kench, 2012). Several studies have examined the role of structure on durability during transport (Ford and Kench, 2012). These studies (Chave, 1964; Ford and Kench, 2012) reveal that algae (*Halimeda* and calcareous red algae) were the least durable grain type, and that corals were the most durable grain type. The poor durability of red algae favored their abrasion during

transport, such as movement from the reef margin (red algal rim) across the reef sand apron. On Aranuka, therefore, the high abundance of red algae near the margin may be due to both the close proximity to the source (e.g., location of highest *in situ* production) and poor durability with transport and abrasion.

For comparison, benthic foraminifera grains have been described as relatively susceptible to breakdown (second least durable, after *Halimeda;* Ford and Kench, 2012). In general, this observation predicts that these grains would be preferentially removed with transport (e.g., relative to coral fragments) across the reef sand apron. Nonetheless, results from Aranuka (Fig. 9) show foraminiferal abundance increases towards the platform interior. Beyond multiple sources of *in situ* production across the sand apron, these data may indicate preferential transport of foraminifera towards the platform interior due to lower density or more-transportable shape (Braithwaite, 1973; Kench and McLean, 1996). In the absence of additional data, these factors cannot be isolated.

*Sediment Assemblages*

Carbonate accumulations throughout the stratigraphic record can be classified into two categories: cool-water carbonate accumulations and tropical water carbonate accumulations (Brookfield, 1988; James, 1997). Cool-water carbonate deposition commonly occurs at latitudes > 30°N or 30°S and at water temperatures <20° C, but can occur in low latitudes with upwelling or elevated nutrient levels (Hallock and Schlager, 1986; James, 1997; Schlager, 2005; Westphal et al., 2010; Michel et al., 2011). Upwelling is associated with cool, nutrient-rich waters at the ocean surface, and influences which sediment producers are present (Hallock and Schlager, 1986; Hallock,

2001). Cool-water accumulations typically have little early marine cementation and are dominantly calcite (Lees and Buller, 1972; Nelson, 1988; James, 1997; Schlager, 2005). Cool-water carbonate systems commonly are associated with the heterozoan assemblage; but a heterozoan assemblage does not mean that the sediments represent cool water conditions, as nutrients also play a role (James, 1997). Heterozoan assemblages, which can include foramol carbonates (Lees and Buller, 1972), can be recognized by the presence of abundant bivalves and foraminifera (Lees and Buller, 1972; James, 1997) as well as little to no lime mud.

In contrast, tropical carbonate accumulations generally are constrained within 30°N and 30°S of the equator and are restricted to clear, warm (temperature >22 C°) shallow (<100 m) water high in oxygen but low in nutrients (James, 1997; Schlager, 2005). Tropical carbonate accumulations are most commonly of the photozoan association (Lees and Buller, 1972), dominated by corals and green algae with a variety of skeletal and nonskeletal grains, such as ooids and peloids, and abundant carbonate mud. The photozoan association includes both aragonite and calcite mineralogy.

Although Aranuka atoll is equatorial (and includes an average annual SST of 27° C), in some regards, sediments comprise what could be considered a heterozoan assemblage (as defined by James, 1997). Sediments on the reef sand aprons are dominantly skeletal grains of red algae, benthic foraminifera, and coral, as well as moderate amounts of bivalve fragments. Sediments on reef sand aprons also lack mud, ooids, peloids, and have very little to almost no green algae (e.g., *Halimeda*), which are common elements on other isolated platforms (Halley and Harris, 1979; Budd and Land,

1990; Rankey et al., 2011) and would be expected to be associated with tropical water accumulations and the photozoan association.

The sediment association on Aranuka is interpreted to reflect its equatorial location, with upwelling that may increase nutrient levels in shallow waters (Wyrtki and Eldin, 1982). Other modern tropical carbonate systems that comprise a heterozoan assemblage include the Yucatan shelf of Mexico, and the northwest African shelf of Mauritania (Summerhayes et al., 1976; Westphal et al., 2010), both of which also are characterized by cool nutrient-rich water upwelling.

*Comparison with Ancient Analogs*

Reef sand aprons form important stratigraphic and geomorphic components of carbonate platforms and rimmed shelves throughout geologic time. Although some ancient platforms include nonactualistic elements (e.g., slope microbial boundstone, Della Porta et al., 2004, Collins et al., 2006; nonraised reef system, Ward et al., 1986), reef sand aprons are evident in numerous geologic systems, including examples from the Devonian (Stauffer, 1968; Playford, 1980, Playford, 1984), Pennsylvanian–Permian (Ruppel and Ward, 2013), Cretaceous (Enos, 1977; Eberli et al., 1993), Miocene (Grotsch and Mercadier, 1999; Neuhaus et al., 2004), and Quaternary (Montaggioni, 2005). Thus, at a broad scale, the geomorphic patterns and facies belts present on Aranuka Atoll are comparable to those of many ancient carbonate platforms (e.g., Leonardian platforms of the Permian Basin, the Maiella platform of Central Italy, and the Malampaya buildup of the Philippines).

Similarly, sedimentological trends are broadly consistent. In many ancient examples, as on Aranuka, sediment fines and becomes less sorted toward the platform interior (Wight and Hardian, 1982; Ward et al., 1986; Masse et al., 1998; Grotsch and Mercadier, 1999; Della Porta et al., 2004; Fournier et al., 2005; Ruppel and Ward, 2013). In one Lower Cretaceous example from Oman, for example, the Shuaiba carbonate platform includes lateral facies changes from the margin to the platform interior, including a textural transition from caprinid-rich grainstone near the margin to *Bacinella* wackestone to packstone near the platform interior (Masse et al., 1998). Similarly, in another well-documented example, the Oligocene strata of Malampaya (South China Sea) includes a lateral transition from coral-foraminiferal-coralline algal grainstone-floatstone near the margin, to mud-rich foraminifera-*Halimeda* floatstone towards the platform interior (Fournier et al., 2005). Finally, in an example from the Middle Triassic Latemar Massif platform of northern Italy, the margin is characterized by reefal boundstone that transitions platformward into a grainstone to packstone (Egenhoff et al., 1999), representing what could be considered an intertidal reef sand apron environment. Further towards the platform interior, the grainstone to packstone transitions into a wackestone to packstone (Egenhoff et al., 1999), illustrating a fining trend from the platform margin towards the platform interior.

Collectively, the sedimentological and geomorphological trends present on Aranuka's reef sand aprons are broadly comparable to those present in ancient platforms. Even though grain size, type, and sorting control depositional porosity (Beard and Weyl, 1973; Pryor, 1973; Nelson, 1994), few studies of ancient analogs examine these sedimentological and geomorphological patterns quantitatively. Although not a perfect

analog for all systems, the results of this study may provide insights useful for prediction of changes in depositional grain size and texture (which control depositional porosity and permeability) from the reef margin to the lagoon of ancient isolated platform systems.

## Conclusions

This study explored reef sand apron dynamics, and integrated field, laboratory, and modeling approaches to examine the sedimentology and physical oceanographic processes of a Holocene reef sand apron on Aranuka Atoll. Understanding the depositional variability in sedimentology and geomorphology of this Holocene reef sand apron provided insights for predicting spatial variability in depositional porosity and permeability.

The results reveal trends in hydrodynamics, geomorphology, and sedimentology from the margin to the platform interior. Hydrodynamically, this tide-modulated, wave-influenced system includes dominant on-platform current that favored the formation of the broad northern reef sand apron, which at >2 km, is one of the widest in the world. Water flooding the atoll from this dominant on-platform flow on the northern margin is interpreted to exit the atoll on the southern margin. Similarly, the dominant on-platform current and platformward decrease in energy across the broad reef sand apron led to systematic changes in grain type, size, and sorting; specifically, sediments transition from well-sorted, coral-red algal, coarse sand and gravel (>1 mm) near the reef margin to poorly sorted, foraminifera-rich, medium sand (~0.5 mm) toward the lagoon. The

sediment assemblage present on Aranuka Atoll, interpreted as heterozoan, most likely reflects equatorial upwelling.

Collectively, the results of this study illustrate that selective winnowing and differentiation of sediment size, type, and sorting (which control depositional porosity and permeability) and the nature and scale of geomorphic elements are linked closely to the hydrodynamics across the platform. The results provide a more rigorous predictive conceptual model for the sedimentological and geomorphic characteristics and dynamics of platform-top reef sand aprons, which may be illustrative for understanding such subsurface reservoir analogs as: 1) Lower Cretaceous Shuaiba carbonate platform of Oman; 2) Miocene Malampaya Buildup of the Philippines; and 3) Middle Triassic Latemar Massif platform of northern Italy.

**References**


BARSTOW, S.F., AND HAUG, O., 1994, The wave climate of the Southwest Pacific: SOPAC (Pacific Islands Applied Geoscience Commission) technical report, 206, p. 7.

BEARD, D.C., AND WEYL, P.K., 1973, Influence of texture on porosity and permeability on unconsolidated sand: American Association of Petroleum Geologists, Bulletin, v. 57, p. 348-369.

BLOTT, S. J., AND PYE, K., 2001, Gradistat: A grain-size distribution and statistics package for the analysis of unconsolidated sediments: Earth Surface Processes and Landforms, v. 26, p. 1237–1248.

BRAITHWAITE, C.J.R., 1973, Settling behaviour related to sieve analysis of skeletal sands: Sedimentology, v. 20, p. 251-262.

BRANDER, R.W., KENCH, P.S., AND HART, D.E., 2004, Spatial and temporal variations in wave characteristics across a reef platform, Warraber Island, Torres Strait, Australia: Marine Geology, v. 207, p. 169–184.

BROOKFIELD, M.E., 1988, A mid-Ordovician temperate carbonate shelf – the Black River and Trenton Limestone Groups of southern Ontario, Canada: Sedimentary Geology, v. 60, p. 137–154.

BUDD, D.A., AND LAND, L.S., 1990, Geochemical imprint of meteoric diagenesis in Holocene ooid sands, Schooner Cays, Bahamas: correlation of calcite cement geochemistry with extant groundwaters: Journal of Sedimentary Petrology, v. 60, p. 361–378.

CHAVE, K, 1964, Skeletal durability and preservation, *in* J. Imbrie and N.D. Newell (Eds.), Approaches to Paleoecology: Wiley, New York, 377-387 p.

CHAVEZ, F.P., STRUTTON, P.G., FRIEDERICH, G.E., FEELY, R.A., FELDMAN, G.C., FOLEY, D.G., AND MCPHADEN, M.J., 1999, Biological and chemical response of the equatorial Pacific Ocean to the 1997-98 El Niño: Science, v. 286, p. 2126-2131.

COASTAL DATA INFORMATION PROGRAM (CDIP), SCRIPPS Institute of Oceanography, 2012: Available at http://cdip.ucsd.edu/ (last accessed 27 May 2013).

COLLINS, J.F., KENTER, J.A.M., HARRIS, P.M., KUANYSHEVA, G., FISCHER, D. J., AND STEFFEN, K.L., 2006, Facies and reservoir-quality variations in the late Visean to Bashkirian outer platform, rim, and flank of the Tengiz buildup, Precaspian Basin, Kazakhstan, *in* P. M. Harris and L. J. Weber, eds., Giant hydrocarbon reservoirs of the world: From rocks to reservoir characterization and modeling: American Association of Petroleum Geologists, Memoir 88/Society for Sedimentary Geology, Special Publication, p. 55–95.

DELLA PORTA, G., KENTER, J.A.M., AND BAHAMONDE, J.R., 2004, Depositional facies and stratal geometry of an Upper Carboniferous prograding and aggrading high-relief carbonate platform (Cantabrian Mountains, N Spain): Sedimentology, v. 51, p. 267–295.

DHI WATER AND ENVIRONMENT, 2007, MIKE 21 Hydrodynamic Model User Guide: Available from DHI Water and Environment, Denmark.

DUNHAM, R.J., 1962, Classification of carbonate rocks according to depositional texture: American Association of Petroleum Geologists, Memoir 1, p. 108- 121.

EBERLI, G.P., BERNOULLI, D., SANDERS, D., AND VECSEI, A., 1993, From aggradation to progradation: the Maiella platform (Abruzzi, Italy), *in* J. T. Simo, R. W. Scott, and J.-P. Masse, eds., Cretaceous carbonate platforms: American Association of Petroleum Geologists, Memoir 56, p. 213–232.

EGENHOFF, S. O., PETERHÄNSEL, A., BECHSTÄDT, T., ZÜHLKE, R., AND GRÖTSCH, J., 1999, Facies architecture of an isolated carbonate platform: tracing the cycles of the Latemar (Middle Triassic, northern Italy): Sedimentology, v. 46, p. 893-912.

ENOS P., 1977, Tamabra Limestone of the Poza Rica trend. Cretaceous, Mexico, in Deep-water carbonate environments: Society for Sedimentary Geology, Special Publication 25, p. 273-314.

FOURNIER, F., BOROGOMANO, J., AND MONTAGGIONI, L.F., 2005, Development patterns and controlling factors of Tertiary carbonate buildups: Insights from high-resolution 3D seismic and well data in the Malampaya gas field (offshore Palawan, Philippines): Sedimentary Geology, v. 175, p. 189-215.

FRANK, T.D., AND JELL, J.S., 2006, Recent developments on a nearshore, terrigenous-influenced reef: Low Isles Reef, Australia: Journal of Coastal Research, v. 22, p. 474-386.

FOLK, R.L., AND WARD, W.C., 1957, Brazos river bar: a study of significance of grain size parameters: Journal of Sedimentary Petrology, v. 27, p. 3–26.

FOLK, R.L., 1962, Spectral subdivision of limestone types, *in* W. E. Ham, ed., Classification of carbonate rocks—a symposium: American Association of Petroleum Geologists, Memoir 1, p. 62–84.

FORD, M.R., AND KENCH, P.S., 2012, The durability of bioclastic sediments and implications for coral reef deposit formation: Sedimentology, v. 59, p. 830-842.

FUJITA, K., OSAWA, Y., KAYANNE, H., IDE, Y., AND YAMANO, H., 2009, Distribution and sediment production of large benthic foraminifers on reef flats of the Majuro Atoll, Marshall Islands: Coral Reefs, v. 28, p. 29-45.

GLOBAL WAVEWATCHIII ARCHIVE, 2013: Available at http://lolabw1.surfline.com/ (last accessed 27 May 2013).

GOURLAY, M.R., 1988, Coral cays: products of wave action and geological processes in a biogenic environment: Proceedings 6th International Coral Reef Symposium, Townsville, Australia, 8–12 August 1988, vol. 2, Symposium Executive Committee, pp. 491– 496.

GROTSCH, J., AND MERCADIER, C., 1999, Integrated 3-D reservoir modeling based on 3-D seismic: the Tertiary Malampaya and Camago buildups, offshore Palawan, Philippines: American Association of Petroleum Geologists, Bulletin, v. 83, p. 1703–1728.

HALLEY, R.B., AND HARRIS, P.M., 1979, Fresh-water cementation of a 1,000-year old oolite: Journal of Sedimentary Petrology, v. 49, p. 969–988.

HALLOCK P., AND SCHLAGER, W., 1986, Nutrient excess and the demise of coral reefs and carbonate platforms: Palaios, v. 1, p. 389–398.

HALLOCK, P., 2001, Coral reefs, carbonate sediments, nutrients, and global change, *in* Stanley GD (ed) The history and sedimentology of ancient reef systems: Kluwer Academic/Plenum Publishers: New York, 387–427 p.

HANDFORD, C.R., AND LOUCKS, R.G., 1993, Carbonate depositional sequences and systems tracts—Responses of carbonate platforms to relative sealevel changes, *in*

Loucks, R., and Sarg, R., eds., Recent advances and applications of carbonate sequence stratigraphy: American Association of Petroleum Geologists, Memoir 57, p. 3-41.

HARRIS, D., WEBSTER, J., DE CARLI, E., AND VILA-CONCEJO, A., 2011, Geomorphology and morphodynamics of a sand apron, One Tree Reef, Southern Great Barrier Reef: Journal of Coastal Research, p. 190-194.

HARNEY, J. N., AND FLETCHER III, C. H., 2003, A budget of carbonate framework and sediment production, Kailua Bay, Oahu, Hawaii: Journal of Sedimentary Research, v. 73, p. 856-868.

HART, D.E., AND KENCH, P.S., 2007, Carbonate production of an emergent reef platform, Warraber Island, Torres Strait, Australia: Coral Reefs, v. 26, p. 53-68.

HINE, A.C., 1977, Lily Bank, Bahamas: history of an active oolite sand shoal: Journal Sedimentary Petrology, v. 47, p. 1554-1581.

HINE, A.C., AND NEUMANN, A.C., 1977, Shallow carbonate bank-margin growth and structure, Little Bahama Bank, Bahamas: American Association of Petroleum Geologists, Bulletin, v. 61, p. 376-406.

JAMES, N. P., 1983, Reef environment, *in* Scholle, P.A., Bebout, D.G., and Moore, C.H. eds., Carbonate Depositional Environments: American Association of Petroleum Geologists, Memoir 33, p. 345-440.

JAMES, N.P., 1997, The cool-water carbonate depositional realm, *in* James NP, Clarke J (eds) Cool-water Carbonates, Society for Sedimentary Geology, Special Publication, v. 56, p 1–20.

KENCH, P.S., 1998a, Physical processes in an Indian Ocean atoll: Coral Reefs, v. 17, p. 155–168.

KENCH, P.S., 1998b, Physical controls on development of lagoon sand deposits and lagoon infilling in an Indian Ocean atoll: Journal of Coastal Research, v. 14, p. 1014–1024.

KENCH, P.S., 1998c, A currents of removal approach for interpreting carbonate sedimentary processes: Marine Geology, v. 145, p. 197–223.

KENCH, P. S., AND MCLEAN, R.F., 1996, Hydraulic characteristics of bioclastic deposits: new possibilities for environmental interpretation using settling velocity fractions: Sedimentology, v. 43, p. 561-570.

KENCH, P. S., AND BRANDER, R.W., 2006, Wave processes on coral reef flats: implications for reef geomorphology using Australian case studies: Journal of Coastal Research, v. 221, p. 209-223.

LEES, A., AND BULLER, A.T., 1972, Modern temperate water and warm water shelf carbonate sediments contrasted: Marine Geology, v. 13, M67–M73.

MAIKLEM, W.R., 1968, Some hydraulic properties of bioclastic carbonate grains: Sedimentology, v. 10, p. 101-109.

MARSHALL, J.F., AND DAVIES, P.J., 1982, Internal structure and Holocene evolution of One Tree Reef, southern Great Barrier Reef: Coral Reefs, v. 1, pp. 21–28.

MASSE, J. P., BORGOMANO, J., AND AL MASKIRY, S., 1998, A platform-to-basin transition for lower Aptian carbonates (Shuaiba Formation) of the northeastern Jebel Akhdar (Sultanate of Oman): Sedimentary Geology, v. 119, p. 297-309.

MAXWELL, W.G.H., JELL, J.S., AND MCKELLER, R.G., 1964, Differentiation of carbonate sediments in the Heron Island reef: Journal of Sedimentary Petrology, v. 34, p. 294–308.

MICHEL, J., VICENS, G.M., AND WESTPHAL, H., 2011, Modern Heterozoan Carbonates from A Eutrophic Tropical Shelf (Mauritania): Journal of Sedimentary Research, v. 81, p. 641-655.

MONTAGGIONI, L.F., 2005, History of Indo-Pacific coral reef systems since the last glaciation: development patterns and controlling factors: Earth Science Reviews, v. 71, p. 1–75.

MUNK, W.H., AND SARGENT, M.S., 1954. Adjustment of Bikini Atoll to ocean waves: U.S. Geological Survey Professional Paper, v. 260-C, p. 275–280.

NELSON, C.S., KEANE, S.L., AND HEAD, P.S., 1988, Non-tropical carbonate deposits on the modern New Zealand shelf: Sedimentary Geology, v. 60, p. 71–94.

NELSON, P. H., 1994, Permeability-porosity relationships in sedimentary rocks: Log Analyst, v. 35, p. 38-38.

NEUHAUS, D., BORGOMANO, J., JAUFFRED, J.C., MERCADIER, C., OLOTU, S., AND GRTSCH, J., 2004, Quantitative Seismic Reservoir Characterization of an Oligocene Miocene Carbonate Buildup: Malampaya Field, Philippines: American Association of Petroleum Geologists, Memoir 81, p. 169-183.

NOAA TIDES AND CURRENTS, 2012, Available at http://tidesandcurrents.noaa.gov (last accessed 28 May 2013).

ODUM, H. T., AND ODUM, E.P., 1955, Trophic structure and productivity of a windward coral reef community on Eniwetok Atoll: Ecology, v. 25, p. 291-320.

PLAYFORD, P. E., 1980, Devonian "Great Barrier Reef" of the Canning Basin, Western Australia: American Association of Petroleum Geologists, Bulletin, v. 64, p. 814-840.

PLAYFORD, P. E., 1984, Platform-margin and marginal-slope relationships in Devonian reef complexes of the Canning Basin, *in* Purcell, P. G., ed., The Canning Basin, Western Australia: Geological Society of Australia and Petroleum Exploration Society of Australia, Canning Basin Symposium, Perth, 189-234 p.

PRYOR, W. A., 1973, Permeability-porosity patterns and variations in some Holocene sand bodies: American Association of Petroleum Geologists, Bulletin, v. 57, p. 162-189.

POMAR, L., 2001, Types of carbonate platforms, a genetic approach: Basin Research, v. 13, p. 313-334.

PURDY, E.G., 1963, Recent calcium carbonate facies of the Great Bahama Bank - 2. Sedimentary facies: Journal of Geology, v. 71, p. 472-497.

PURDY, E.G., AND GISCHLER, E., 2005, The transient nature of the empty bucket model of reef sedimentation: Sedimentary Geology, v. 175, p. 35-47.

RANKEY, E.C., GUIDRY, S.A., REEDER, S.L., AND GUARIN, H., 2009, Geomorphic and sedimentologic heterogeneity along a Holocene shelf margin: Caicos Platform: Journal of Sedimentary Research, v. 79, p. 440–456.

RANKEY, E.C., AND REEDER, S.L., 2010, Controls on platform-scale patterns of surface sediments, shallow Holocene platforms, Bahamas: Sedimentology, v. 57, p. 1545-1565.

RANKEY, E.C., 2011, Nature and stability of atoll island shorelines: Gilbert Island chain, Kiribati, equatorial Pacific: Sedimentology, v. 58, p. 1831-1859.

RANKEY, E.C., AND REEDER, S.L., 2011, Holocene oolitic marine sand complexes of the Bahamas: Journal of Sedimentary Research, v. 81, p. 97-117.

RANKEY, E.C., REEDER S.L., AND GARZA-PEREZ, J.R., 2011, Controls on links between geomorphology and surface sedimentological variability: Aitutaki and Maupiti Atolls, South Pacific Ocean: Journal of Sedimentary Research, v. 81, p. 885–900.

RANKEY, E.C., and GARZA-PEREZ, J.R., 2012, Seascape metrics of shelf-margin reefs and reef sand aprons of Holocene carbonate platforms: Journal of Sedimentary Research, v. 85, p. 53-71.

READ J.F., 1985, Carbonate platform facies models**:** American Association of Petroleum Geologists, Bulletin, v. 69, p. 1-21.

REEDER, S.L., AND RANKEY, E.C., 2009, Controls on morphology and sedimentology of carbonate tidal deltas, Abacos, Bahamas: Marine Geology, v. 267, p. 141-155.

RICHMOND, B.M., 1993, Reconnaissance geology of the Gilbert Group, western Kiribati: SOPAC (Pacific Islands Applied Geoscience Commission) Technical Report 77, p. 65.

RUPPEL, S.C, AND WARD, B.W., 2013, Outcrop-based characterization of the Leonardian carbonate platform in west Texas: Implications for sequence-stratigraphic styles in the Lower Permian: American Association of Petroleum Geologists, Bulletin, v. 97, p. 223-250.

SACHET, M.H., 1957, Climate and meteorology of the Gilbert Islands: Atoll Research Bulletin, v. 60, p. 20.

SCOFFIN, T.P., AND TUDHOPE, A.W., 1988, Shallowing-upwards sequences in reef lagoon sediments: examples from the Holocene of the Great Barrier Reef of Australia and the Silurian of Much Wenlock, Shropshire, England: 6th International Coral Reef Symposium, Australia, Proceedings, v. 3, p. 479–484.

SHINN, E. A., 1963, Formation of spurs and grooves on the Florida reef track: Journal of Sedimentary Petrology, v. 33, p. 291-303.

SCHLAGER, W., 2005, Carbonate Sedimentology and Sequence Stratigraphy: Society for Sedimentary Geology, Concepts in Sedimentology and Paleontology, no. 8, 24 p.

SORBY, H.C., 1879, The Structure and Origin of Limestones: Proceedings of the Geological Society of London, v. 35, p. 56-95.

STAUFFER, K.W., 1968, Silurian-Devonian reef complex near Nowshera, west Pakistan: Geological Society of America, Bulletin, v. 79, p. 1331-1350.

STODDART, D.R., 1969, Ecology and morphology of recent coral reefs: Biological Reviews, v. 44, p. 433-489.

SUMMERHAYES, C.P., MILLIMAN, J.D., BRIGGS, S.R., BEE, A.G., AND HOGAN, C., 1976, Northwest African shelf sediments: influence of climate and sedimentary processes: The Journal of Geology, v. 84, p. 277–300.

SURFLINE/WAVETRAK, INC., 2013, Available at http://lolabw1.surfline.com/ (last accessed 28 May 2013).

TUDHOPE, A.W., 1989, Shallowing-upwards sedimentation in a coral reef lagoon, Great Barrier Reef of Australia: Journal of Sedimentary Petrology, v. 59, p. 1036–1051.

WARD, R.F., KENDALL, C.G. S.C., AND HARRIS, P. M., 1986, Upper Permian (Guadalupian) facies and their association with hydrocarbons--Permian basin, west Texas and New Mexico: American Association of Petroleum Geologists, Bulletin, v. 70, p. 239-262.

WESTPHAL, H., HALFAR, J., AND FREIWALD, A., 2010, Heterozoan carbonates in subtropical to tropical settings in the present and past: International Journal of Earth Sciences, v. 99, p. 153-169.

WIENS, H.J., 1962, Atoll environment and ecology: Yale University Press, New Haven and London, 45-85 p.

WIGHT, A., AND HARDIAN, D., 1982, Importance of diagenesis in carbonate exploration and production, Lower Batu Raja Carbonates, Krisna Field, Java Sea: Indonesian Petroleum Association, Proceedings 11th Annual Convention, p. 211 – 236.

WILLIAMS, H. D., BURGESS, P. M., WRIGHT, V. P., DELLA PORTA, G., AND GRANJEON, D., 2011, Investigating carbonate platform types: Multiple controls and a continuum of geometries: Journal of Sedimentary Research, v. 81, p. 18-37.

WILSON, J.L., 1975, Carbonate facies in geologic history: Springer-Verlag, New York, 1-19 p.

WOODROFFE, C. D., AND BIRIBO, N., 2011, Atolls, *in* D. Hopley (Eds.), Encyclopedia of Modern Coral Reefs: structure, form and process: The Netherlands: Springer, 51-71 p.

WYRTKI, K., AND G. ELDIN, 1982, Equatorial upwelling events in the central Pacific: Journal of Physical Oceanography, v. 12, p. 984–988.

YAMANO, H., MIYAJIMA, T., AND KOIKE, I., 2000, Importance of foraminifera for the formation and maintenance of a coral sand cay: Green Island, Australia: Coral Reefs, v. 19, p. 51-58.

**Figures**

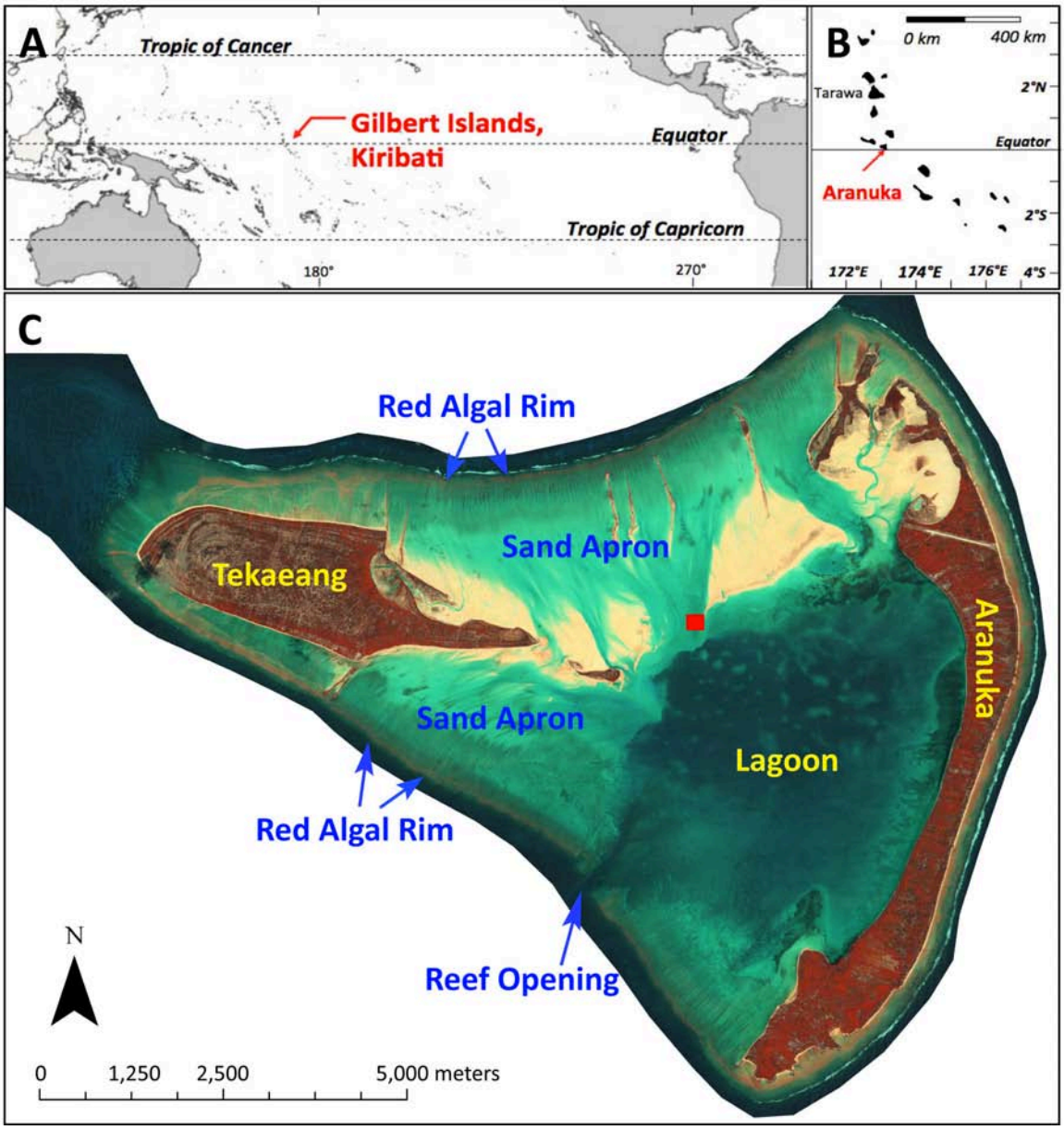


**Fig. 1.** Geographic location and general geomorphology of Aranuka Atoll. A) Location of the Gilbert Islands, Republic of Kiribati in the equatorial Pacific. B) Location of Aranuka Atoll within the Gilbert Chain. C) Remote sensing image of Aranuka atoll. The red square indicates the location of deployment of the *in situ* current meter. Remote sensing image is copyright GeoEye.com.

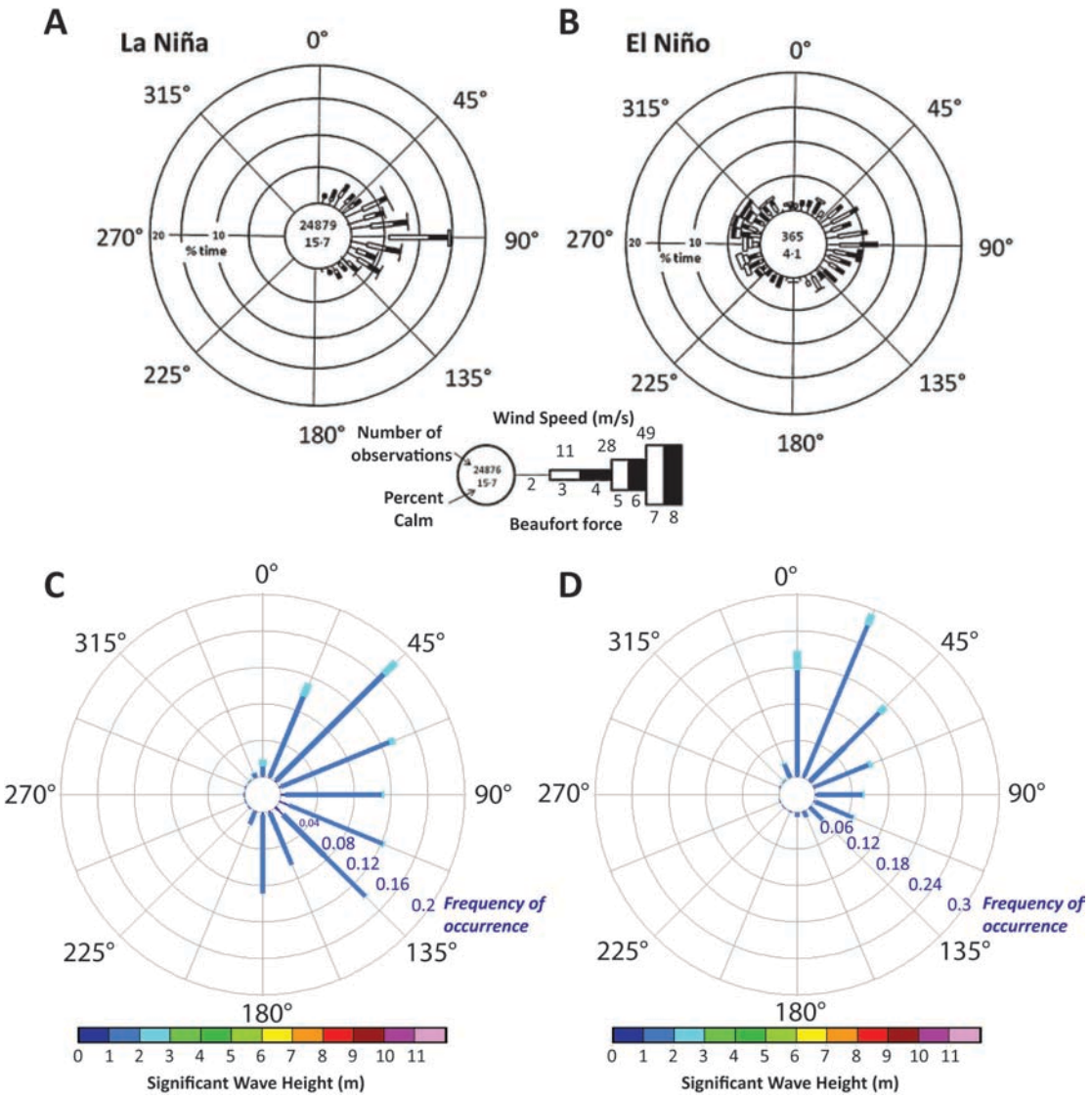


**Fig. 2.** Wind and wave direction and magnitude plots. A and B) Graph of wind magnitude and direction from Tarawa, Republic of Kiribati (Fig. 1B), during both La Niña (A) and El Niño (B) phases (Richmond, 1993). During both La Niña and El Niño phases winds come from the east, but during El Niño phases, strong westerly winds are common. C and D) Plots of wave direction and magnitude from the Marshall Islands (located ~670 km away; data are unavailable for the Republic of Kiribati). These data illustrate the seasonal variability in wave direction between C) April - September 2010 (northern hemisphere summer, 7734 records), and D) October 2010–March 2011 (northern hemisphere winter; 8736 records). The wave direction ranges from the northeast to southeast with a significant wave height that can reach 2 m in the northern hemisphere summer (C) to north-northeast with a significant wave height of 2–3 m (D). Data represent a La Niña phase; El Niño data are unavailable (data from The Coastal Data Information Program (CDIP), Scripps Institution of Oceanography, 2012).

| Simulation | Wind | Tides | Distal Waves |
|---|---|---|---|
| **Description** | MIKE21 Hydrodynamic (HD) simulation run with only wind applied. This simulation generates local wind waves (No tidal or distal wave parameters applied) | MIKE21 Hydrodynamic (HD) simulation run with only tides applied to all four boundary conditions (No distal wave or wind parameters applied) | MIKE21 Hydrodynamic (HD) MIKE 21 simulation run in conjunction with MIKE21 Nearshore Spectral Wave (NSW). Only wave radiation stresses applied (No tide or wind parameters applied) |
| **Inputs: *Basic parameters*** | | | |
| Bathymetry | Unstructured mesh-Aranuka bathymetric grid (50 X 50 m) | Unstructured mesh-Aranuka bathymetric grid (50 X 50 m) | Unstructured mesh-Aranuka bathymetric grid (50 X 50 m) |
| Simulation period | ~24 hours with a time step interval of 5 sec | ~24 hours with a time step interval of 5 sec | ~24 hours with a time step interval of 5 sec |
| Grid Boundary | Program detected from bathymetry (reef margin is ~100 grid cells from the model boundaries to account for the edge effects) | Program detected from bathymetry (reef margin is ~100 grid cells from the model boundaries to account for the edge effects) | Program detected from bathymetry (reef margin is ~100 grid cells from the model boundaries to account for the edge effects) |
| Flood and dry | Drying = 0.1 m Flooding = 0.2 m | Drying = 0.1 m Flooding = 0.2 m | Drying = 0.1 m Flooding = 0.2 m |
| **Inputs: *Hydrodynamic Parameters*** | | | |
| Initial surface elevation | Negative 0.11 m | Negative 0.11 m | Negative 0.11 m |
| Boundary | Constant value = 0 on all four boundaries | NOAA tide data on all four boundaries | Constant value = 0 on all four boundaries |
| Eddy viscosity | Constant value (velocity based) = 0.025 $m^2/s$ | Constant value (velocity based) = 0.025 $m^2/s$ | Constant value (velocity based) = 0.025 $m^2/s$ |
| Resistance | Manning number = 32 | Manning number = 32 | Manning number = 32 |
| Wave radiation | Not applied | Not applied | Wave radiation stresses file (computed using Aranuka bathymetric grid) created by MIKE21 NSW was input into the MIKE21 HD model.<br>Constant in time and space and propagated from north (0°)<br>Wave height = 2 and 4 m<br>Wave Period = 7 and 17 sec |
| Wind Conditions | Constant in time and space<br>Speed set at 10 m/s from east (90°) | Not applied | Not applied |

**Table 1.** Hydrodynamic simulations run by MIKE21 with the detailed input parameters. Only those parameters highlighted in blue vary among simulations.

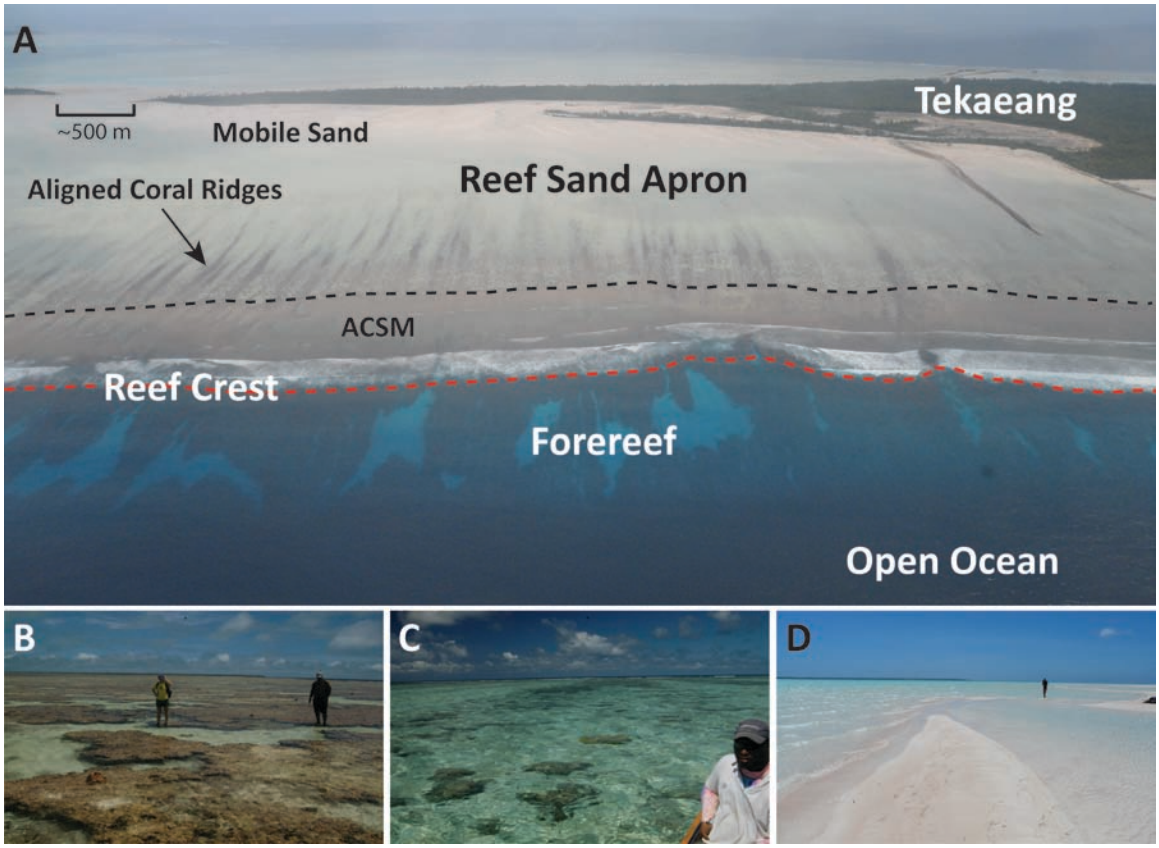


**Fig. 3.** Field photographs illustrating geomorphic variability of Aranuka Atoll. A) Low-angle aerial photo illustrating geomorphic elements of central part of the atoll and the geomorphic subzones within the sand apron. View is towards the south with the scale between islands in the distance. Within 300 m of the margin on the reef sand apron is a subzone of (B) amalgamated to closely spaced microatolls (ACSM), which gradually transition platformward into (C) the aligned coral ridge subzone and (D) the mobile sand subzone. People for scale in B–D.

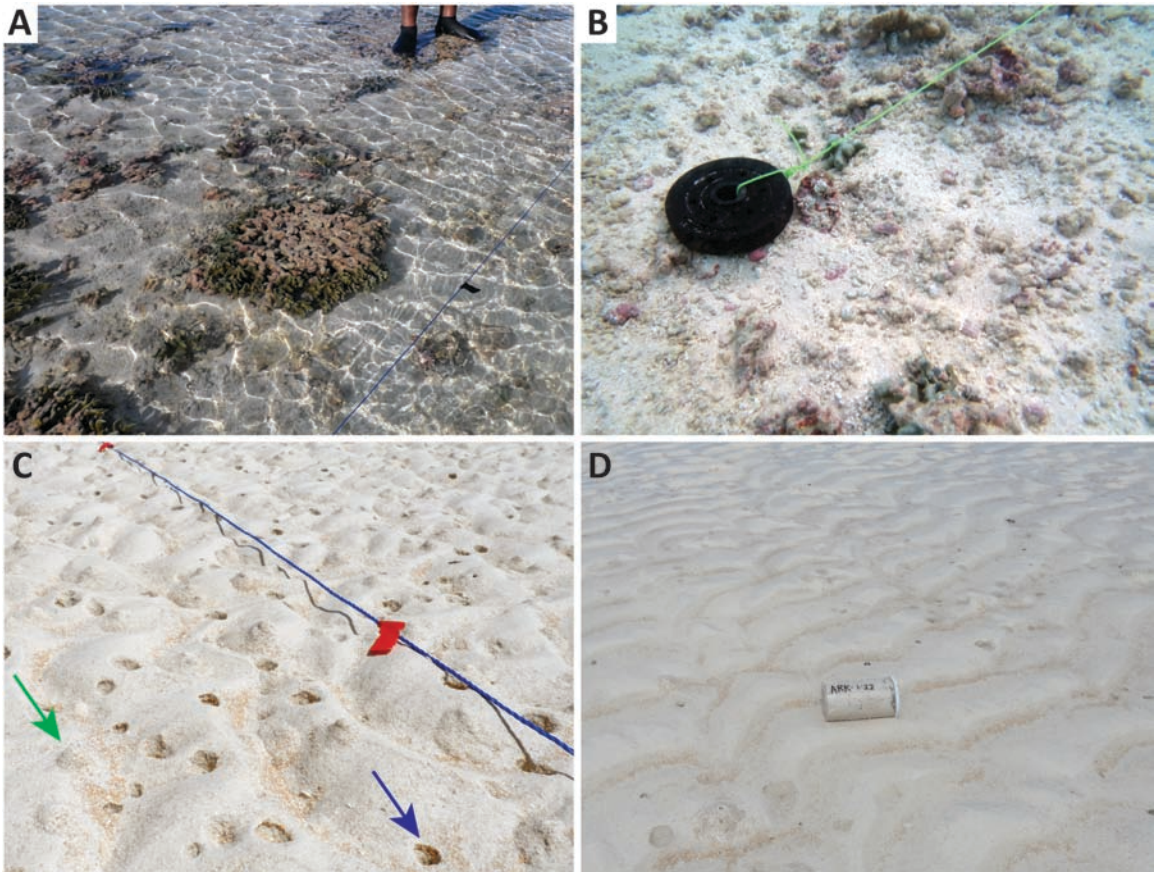


**Fig. 4.** Field photos illustrating variability in bottom types from the Aranuka reef sand apron. A) Coral microatolls. Isolated microatolls, such as this one, are generally ~1 m in diameter and are typically surrounded by a rocky bottom with thin patchy accumulations of sediment. A man's feet serve as a scale (30 cm). B) Sandy rubble to gravel. Much of the coarse rubble debris consists of broken *Heliopora* coral. The weight is 30 cm in diameter, for scale. C) A burrowed, bare sand bottom is common in the most platformward portion of the reef sand aprons. Many burrows are pits (up to 2–3 cm in diameter, blue arrow) and pimple-like mounds (green arrow). There are also relict ripples. Distance between red tape on the line is 1 m. D) Bare sand with flood oriented, sinuous crested 2D ripples. Ripple spacing is ~6 cm and height is ~1cm. Sample vial is 5.4 cm long.

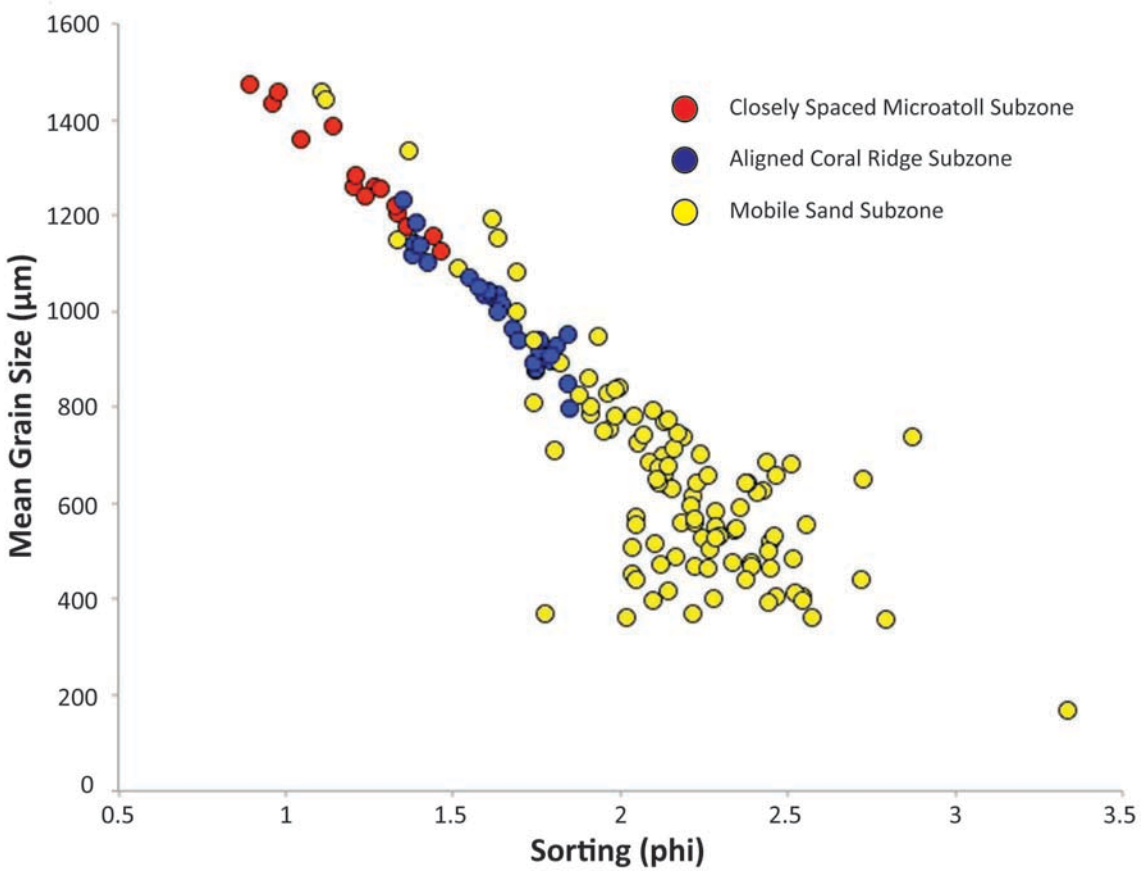


**Fig. 5.** Comparison of granulometric trends of sediment samples among geomorphic subzones from both the northern and southern reef sand aprons (N=146). The samples from each subzone cluster, and there is a clear relationship between mean grain size and sorting among all the subzones.

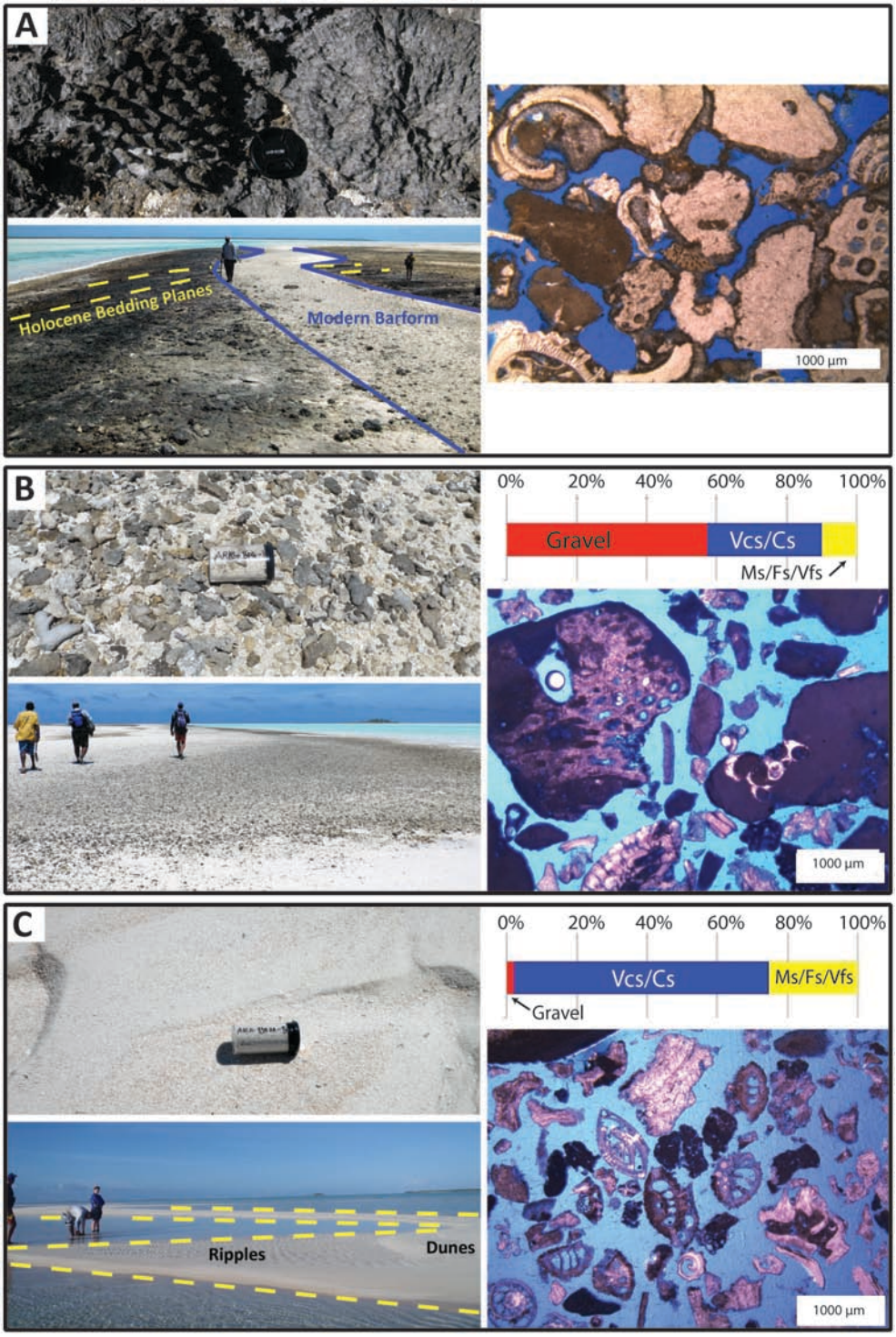


**Fig. 6.** On-platform changes in margin-normal barforms on the northern reef sand apron. Each part shows two photos of the field appearance, as well as grain size distribution and photomicrograph from a representative sample. Abbreviations on grain sizes include: Vcs/Cs is very coarse sand/coarse sand; Ms/Fs/Vfs is medium sand/fine sand/very fine

sand. A) Near the margin, the earlier Holocene rocky barform includes beds (highlighted by yellow) dipping southward (on-platform) as they bend westward; the view is towards the platform interior. The photomicrograph includes cemented coarse skeletal debris that forms the rocky part at the head of the gravel barform. No grain size distribution for this portion of the barform was available due to the lack of unlithified material for sieve analysis. B) Further platformward, the barform includes unlithified sediment including coarse sand and gravel with abundant coral and red algal grains. This very coarse sediment gradationally transitions platformward into a (C) sandy barform, with small dunes and ripples. The photomicrograph includes the abundant coral and foraminiferal fragments, and the finest sediment on the bar form.

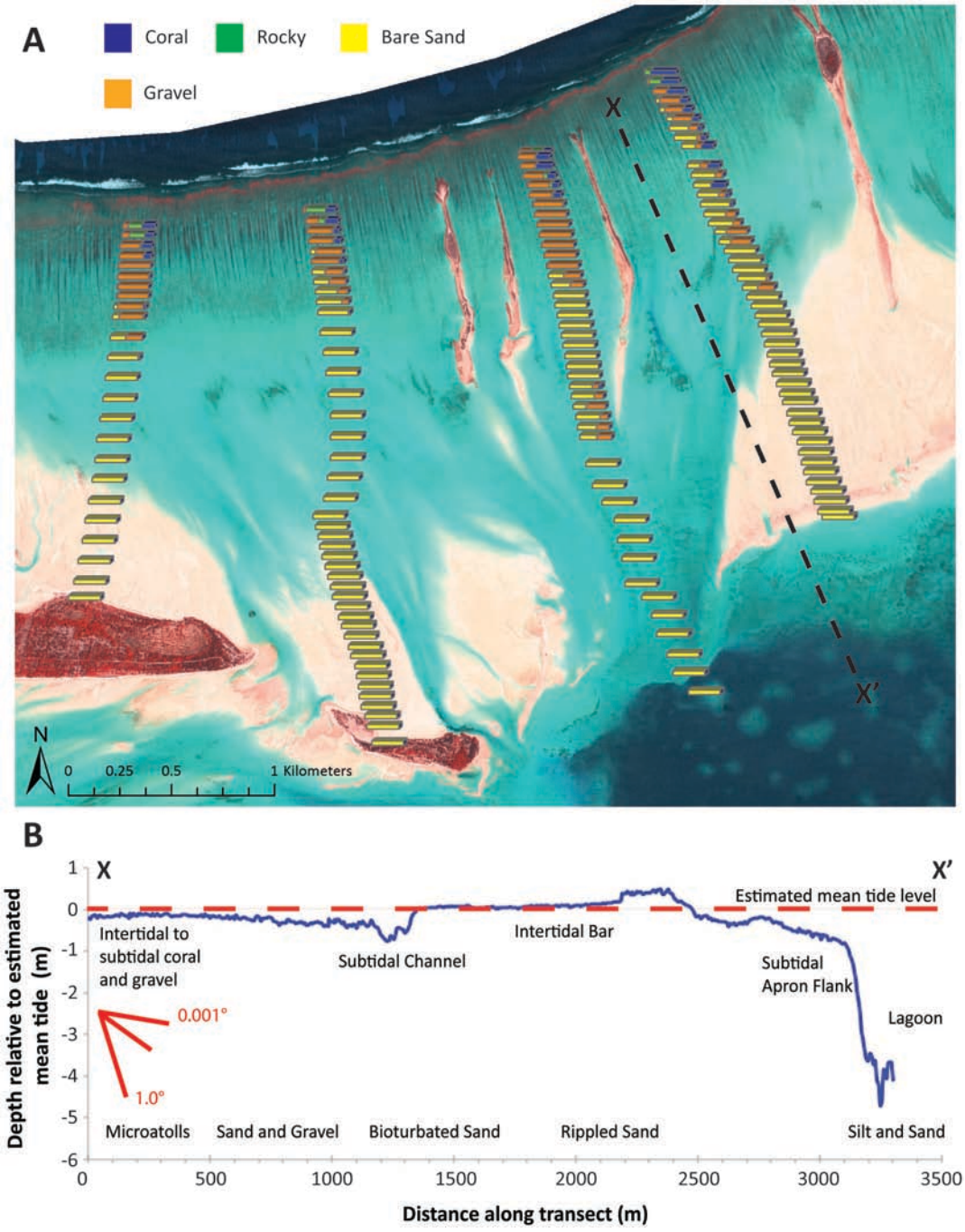


**Fig. 7.** Bottom type and topography on the northern reef sand apron. A) Bottom types are coral-rocky dominated near the margin and transition platformward into bare sand, which includes rippled and burrowed bare sand. Similar trends are present on the southwestern sand apron. B) Topographic cross section of part of the northern reef sand apron (transect begins 500 meters from the margin; X in part A). The sand apron is not a simple homoclinal plane dipping into the lagoon; instead, it includes subtle channels and bars.

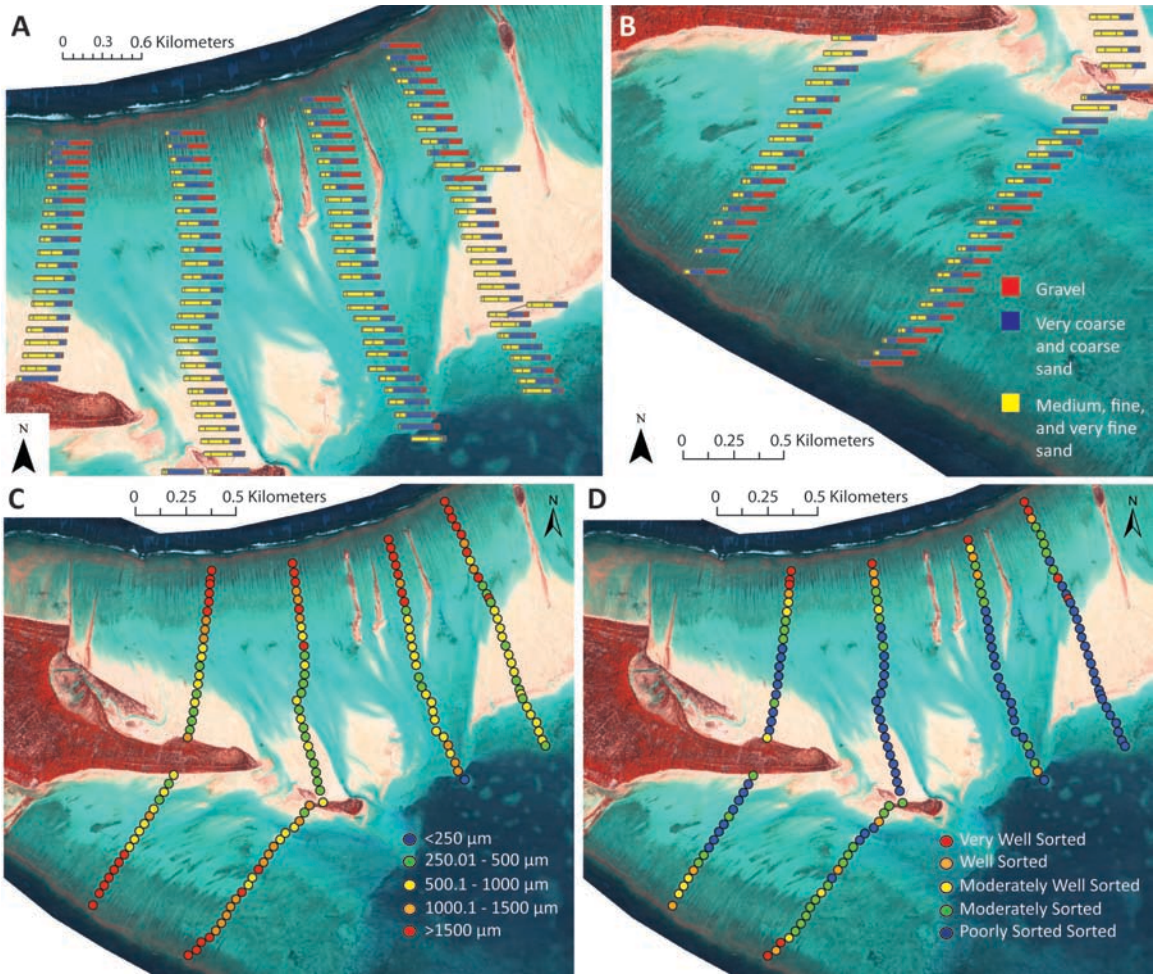


**Fig. 8.** Granulometric characteristics of the northern and southern reef sand aprons. A) Data from the northern reef sand apron. Sediment is dominated by very coarse sand and gravel near the margin, but transitions platformward into finer sand. B) Data from the southern reef sand apron. Here, sediment includes trends in grain size from the margin to the lagoon similar to those on the northern apron. C) Median grain size of reef sand apron surface sediment. The mean sediment size changes from very coarse near the margin to finer, platformward. D) Sorting (Folk and Ward, 1957). In general, sediment is very well sorted (warm colors) near the margin and becomes more poorly sorted (cool colors) toward the platform interior.

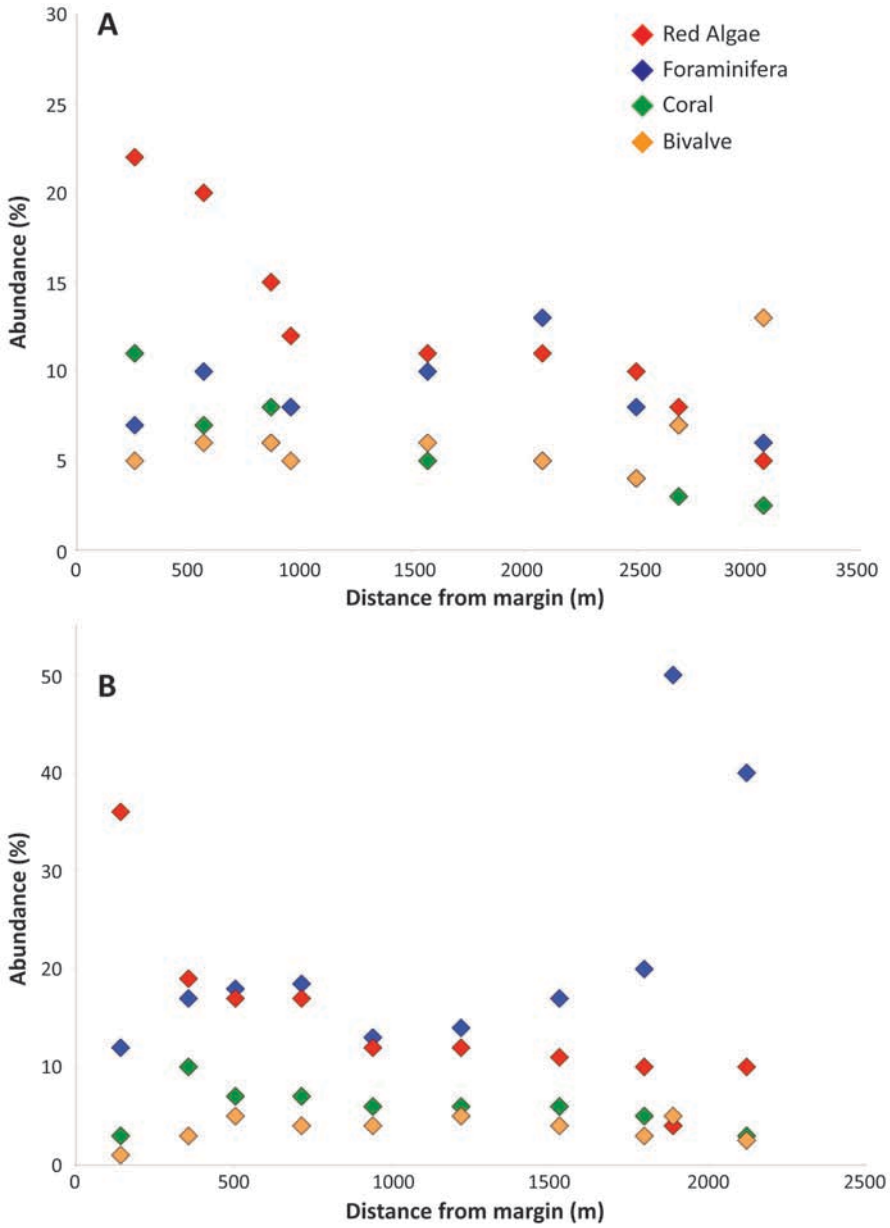


**Fig. 9.** Comparison of the relative abundance of identified grain types from representative sediment transects, from the northern (A) and southern (B) sand apron. All transects show a decrease in abundance of red algae and coral with increasing distance from the margin. Abundance of foraminifera generally increases with distance from the margin.

| Reef Sand Apron Geomorphic Subzones | Distance Relative to Platform Margin | Dominant Bottom Type | Number of Samples | Mean Grain Size (μm) | Mean Sorting (phi) | Dominant Grain Type |
|---|---|---|---|---|---|---|
| Amalgamated- to Closely Spaced-Microatoll | Within ~300 m of Margin | Coral and Rocky | N=15 | Coarse Sand and Gravel; 1286 μm | Very well-sorted; 1.21 ϕ | Red Algae |
| Aligned Coral | Between ~300-700 m of Margin | Gravel | N=27 | Coarse Sand to Gravel; 998 μm | Moderately Sorted; 1.64 ϕ | N/A |
| Mobile Sand | > 700 m from Margin | Burrowed and Rippled Bare Sand | N=104 | Medium to Coarse Sand; 658 μm | Poorly Sorted; 2.15 ϕ | Benthic Foraminifera |

**Table 2.** Comparison of geomorphic, granulometric, and bottom type characteristics from the reef sand apron subzones of Aranuka. The sediment fines and decreases in sorting from the closely spaced- to- amalgamated microatoll subzone to the mobile sand subzone.

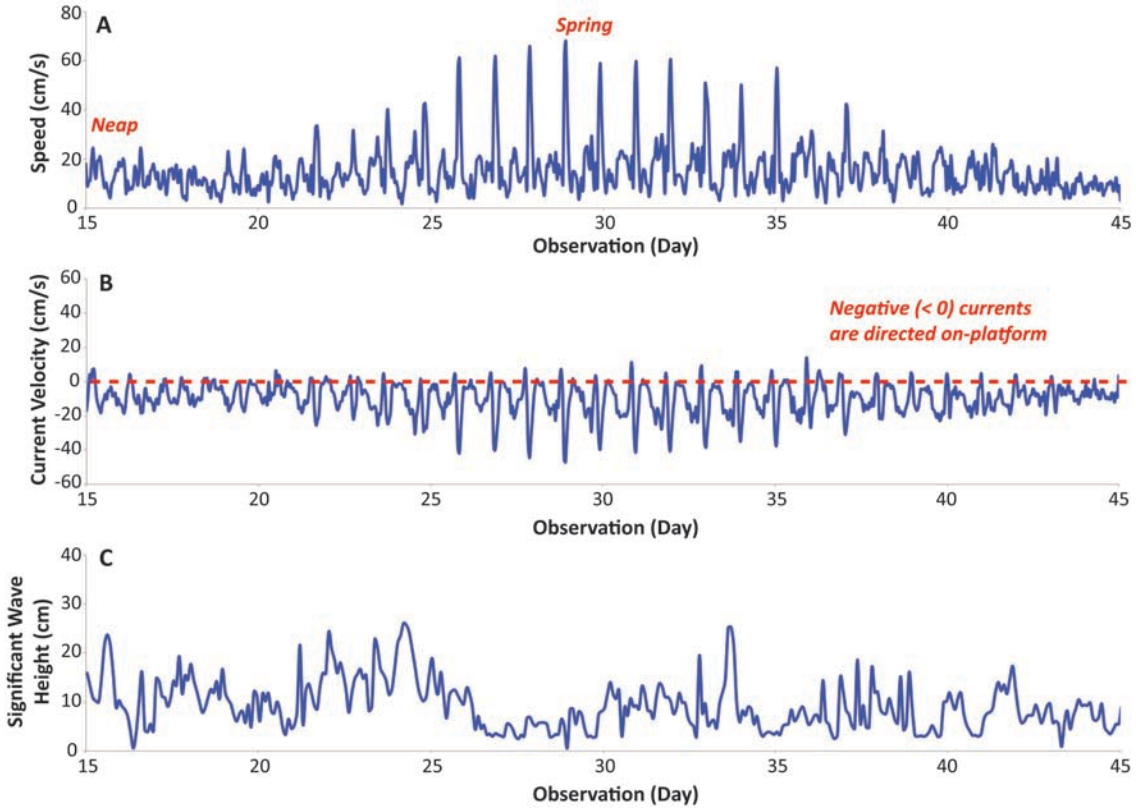


**Fig. 10.** Currents and waves on the northern reef sand apron over a representative 30-day period (see Fig. 1 for deployment location). A) Plot of current speed (cm/s), highlighting both spring and neap tides. During spring tide, current speeds may exceed 60 cm/s, slower than those during neap tide, which may not exceed 25 cm/s. B) Plot displaying the northern component of velocity (cm/s). Negative velocities refer to on-platform (southward) currents; the red dashed line helps distinguish between off-platform flow and on-platform flow. The dominant flow direction is on-platform (velocities <0). C) Plot of significant wave height (cm). The wave height is generally small (<30 cm) on the platform and there is an absence of a correlation between currents and significant wave height.

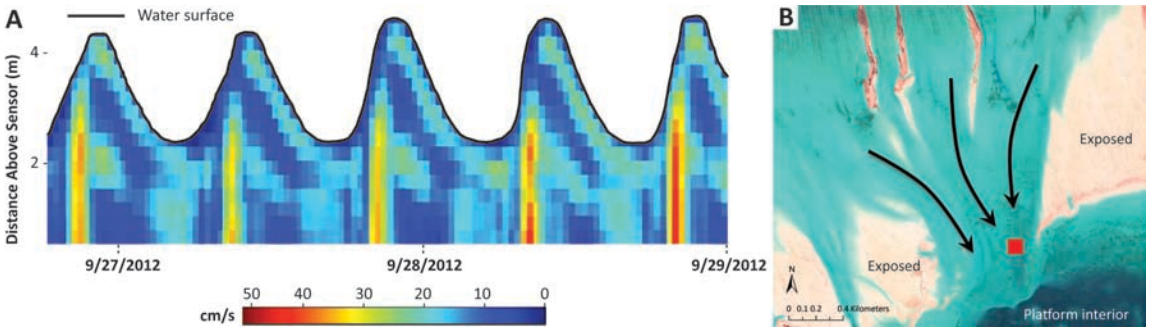


**Fig. 11.** Hydrodynamical data from the *in situ* current meter on the northern reef sand apron. A) Water depth and current speed of a representative (~2 day) interval. On this plot, the data represent the current speed (color coded) with depth (Y-axis, 25 cm resolution), through time (X axis, samples every 30 minutes). As the water level moves up and down with the tide (black line at the top of colored boxes), the current speed changes; the highest flow speeds occur during early rising tide. B) Remote sensing image illustrating the field location of the *in situ* current meter (red box) and the interpreted channel-focused currents during the early stages of flood tide (on-platform flow, towards the bottom of the image).

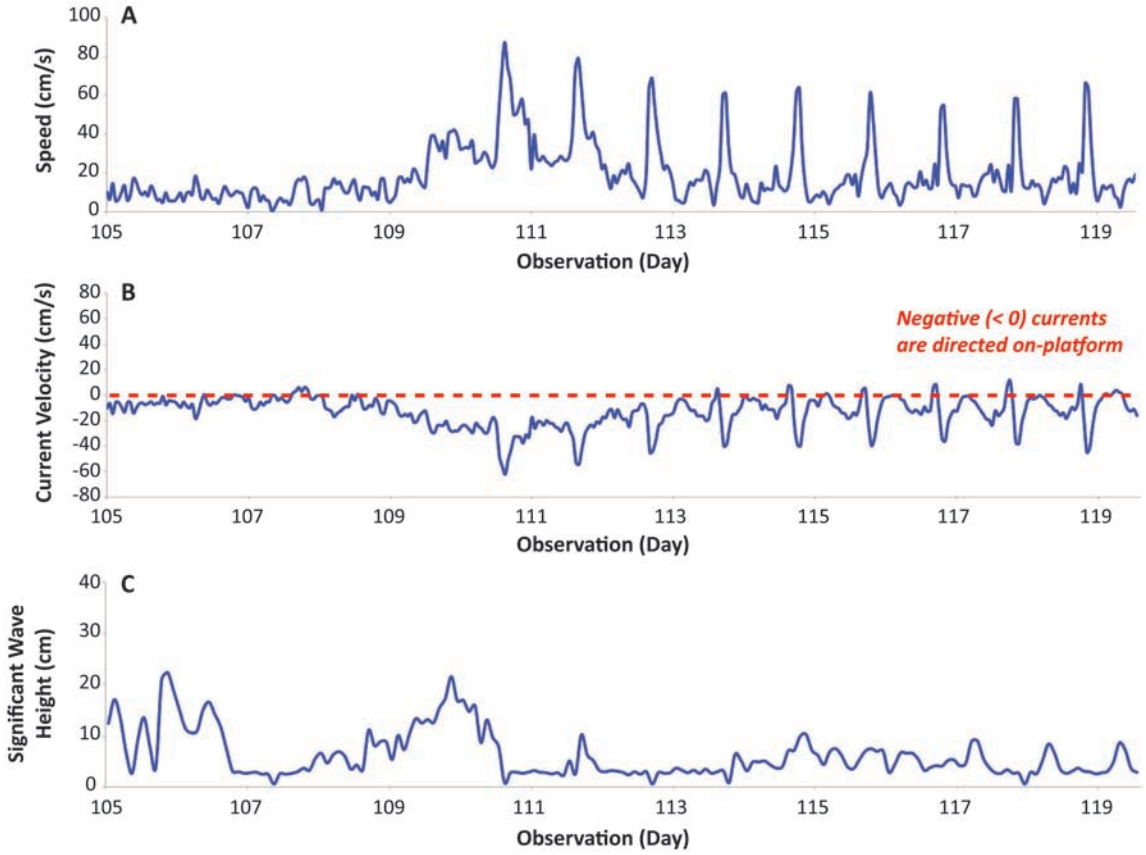


**Fig. 12.** Currents and waves recorded during an event of sustained, elevated on-platform currents, between days 109-113 (October 11–13, 2012). A) Plot of current speed (cm/s). Note that currents reach ~90 cm/s – the highest recorded over the 9 week collection period. B) Plot displaying the northern component of velocity. Negative velocities refer to on-platform (southward) currents. During the event, the dominant flow direction is on-platform. C) Plot illustrating the significant wave height (cm). Waves are not markedly larger during this interval than wave heights of most other times (Figure 10C).

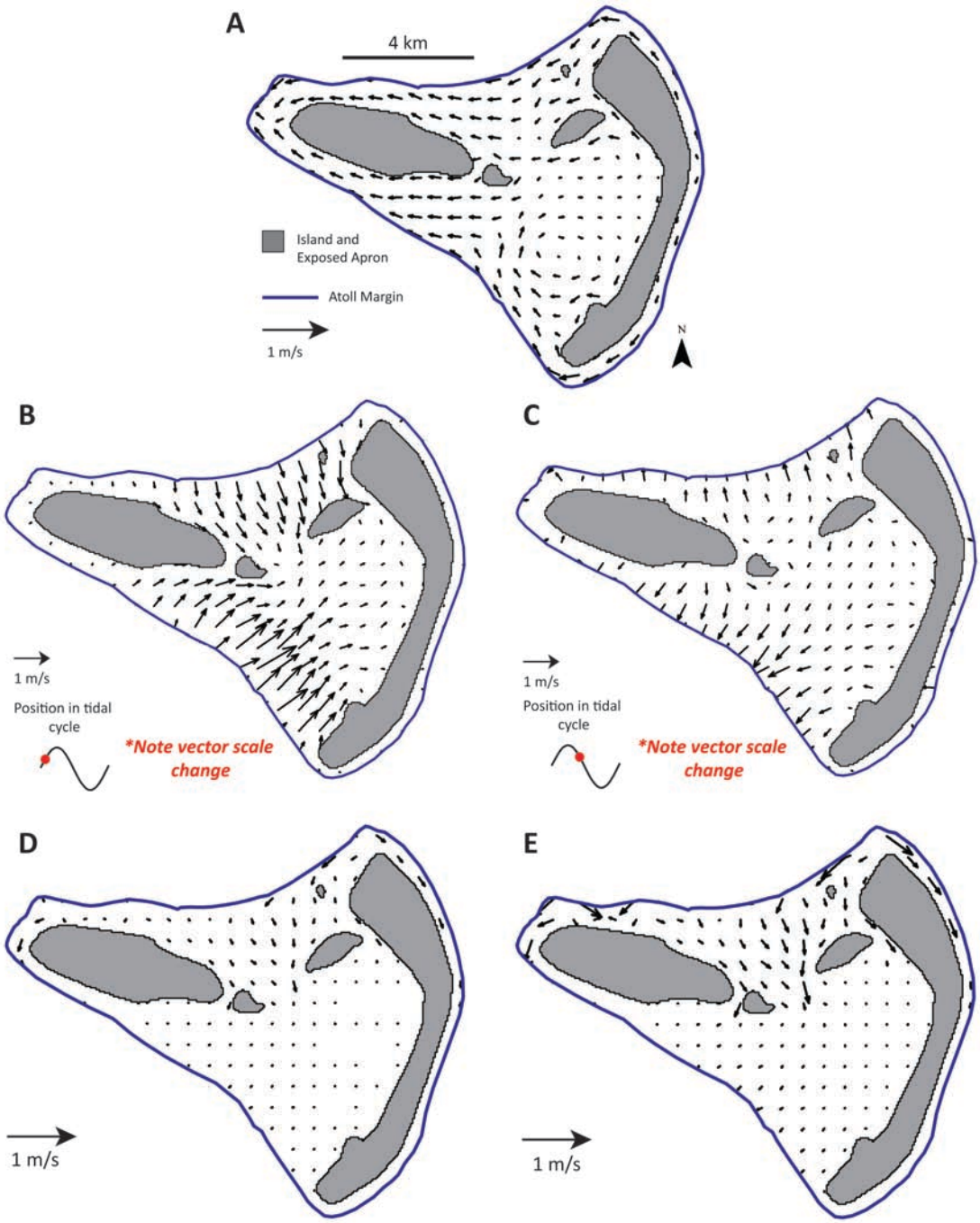


**Fig. 13.** MIKE21 hydrodynamic modeling results. A) Wind simulation with winds generated from the east (90°). Note the dominant unidirectional flow in the direction of wind generation, although several eddies are evident. B and C) Tide simulation results of current patterns with 2.5 m tidal amplitude (B is flood tide, C is ebb tide), and no wind or wave forcing. The vector scale changes between these and all other simulations. These plots show bidirectional flow with much higher velocities than under the other conditions. D and E) Wave simulation with 2 m (D) and 4 m (E) waves generated from the north

(0°); no wind or tides are applied. There is a dominant north-to-south flow, and the elevated flow speeds with the 4 m wave height (compared to the 2 m wave height). Original model outputs are available in appendix A.

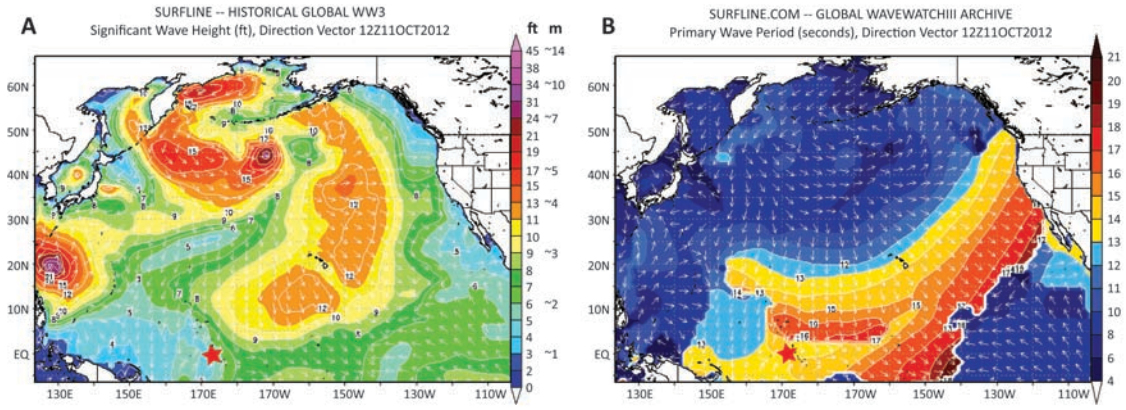


**Fig. 14.** Data from the Global WAVEWATCHIII archive illustrating the impacts of a strong early winter cold front across the north Pacific on October 11th, 2012. These large waves occurred at the same time that the in situ current meter on Aranuka recorded sustained elevated on-platform currents (Figure 12). A) Significant wave height (feet, one foot = 30.5 cm) B) Wave period (seconds). The red star indicates the location of Aranuka Atoll. Data from Surfline.com, copyright 2013 Surfline/Wavetrak, Inc.

## Appendix I – Original MIKE21 Model Outputs

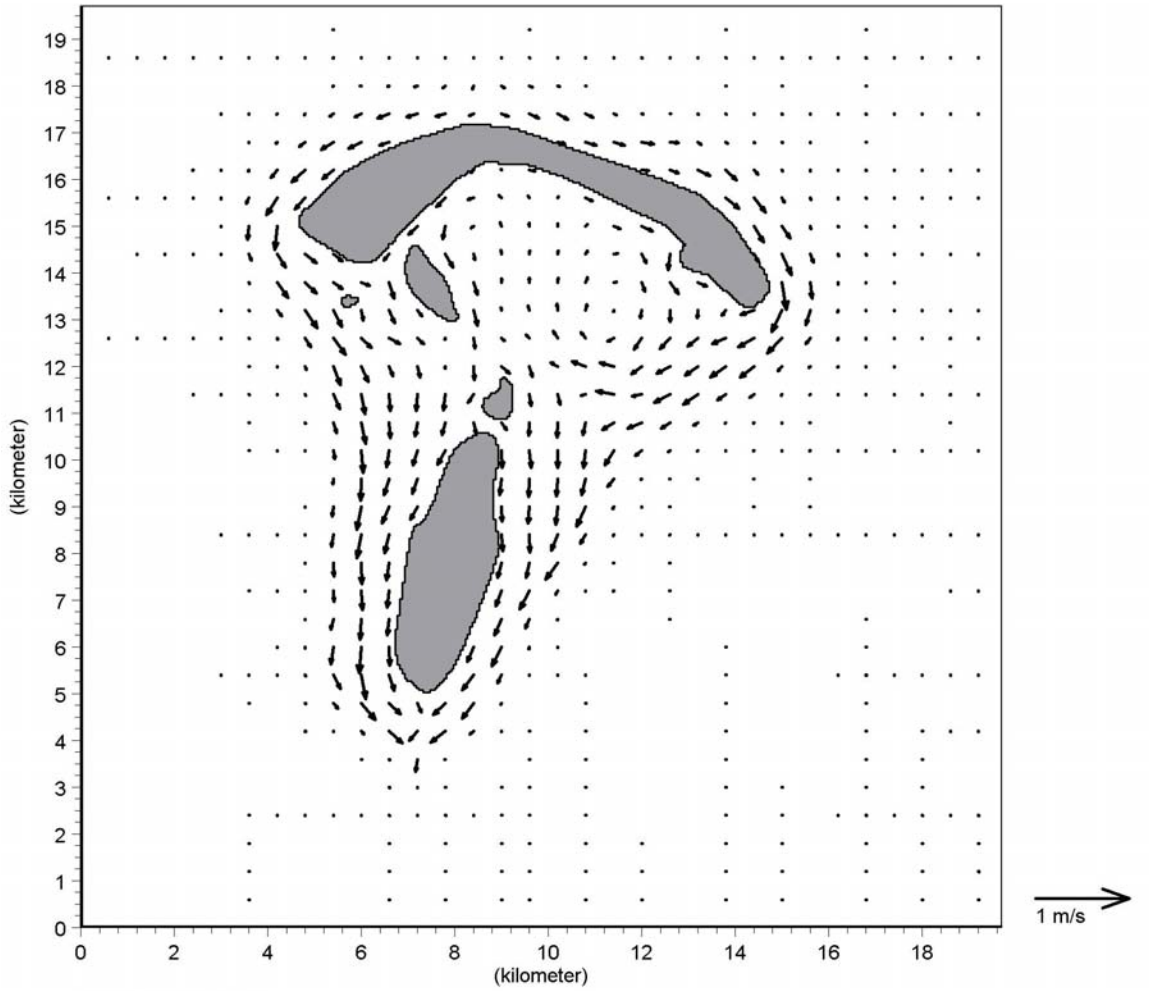


MIKE21 wind simulation with winds generated from the East (90°) at 10 m/s. Note that true north is to the left of the image.

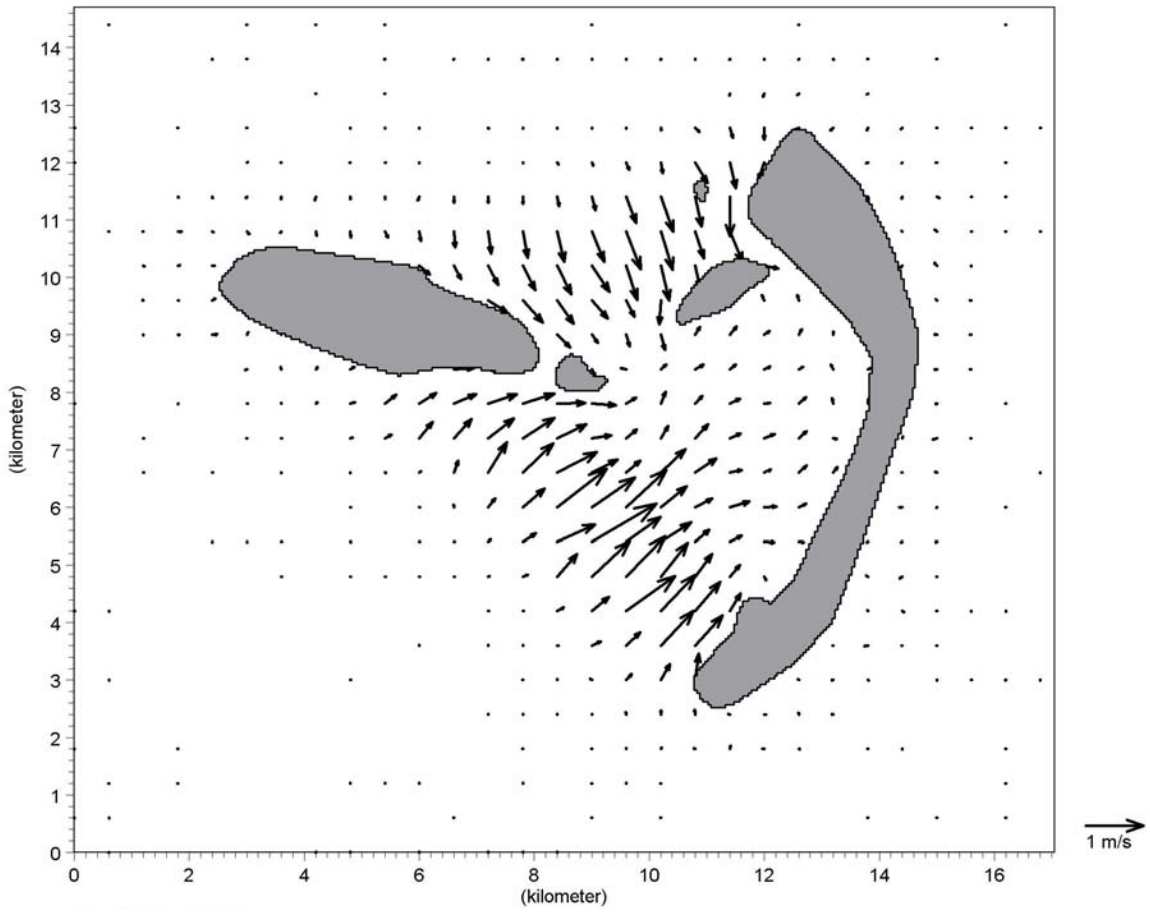


MIKE21 tide simulation with 2.5 m amplitude tides. Image generated during flood stage of tidal cycle. True north is at the top of the image.

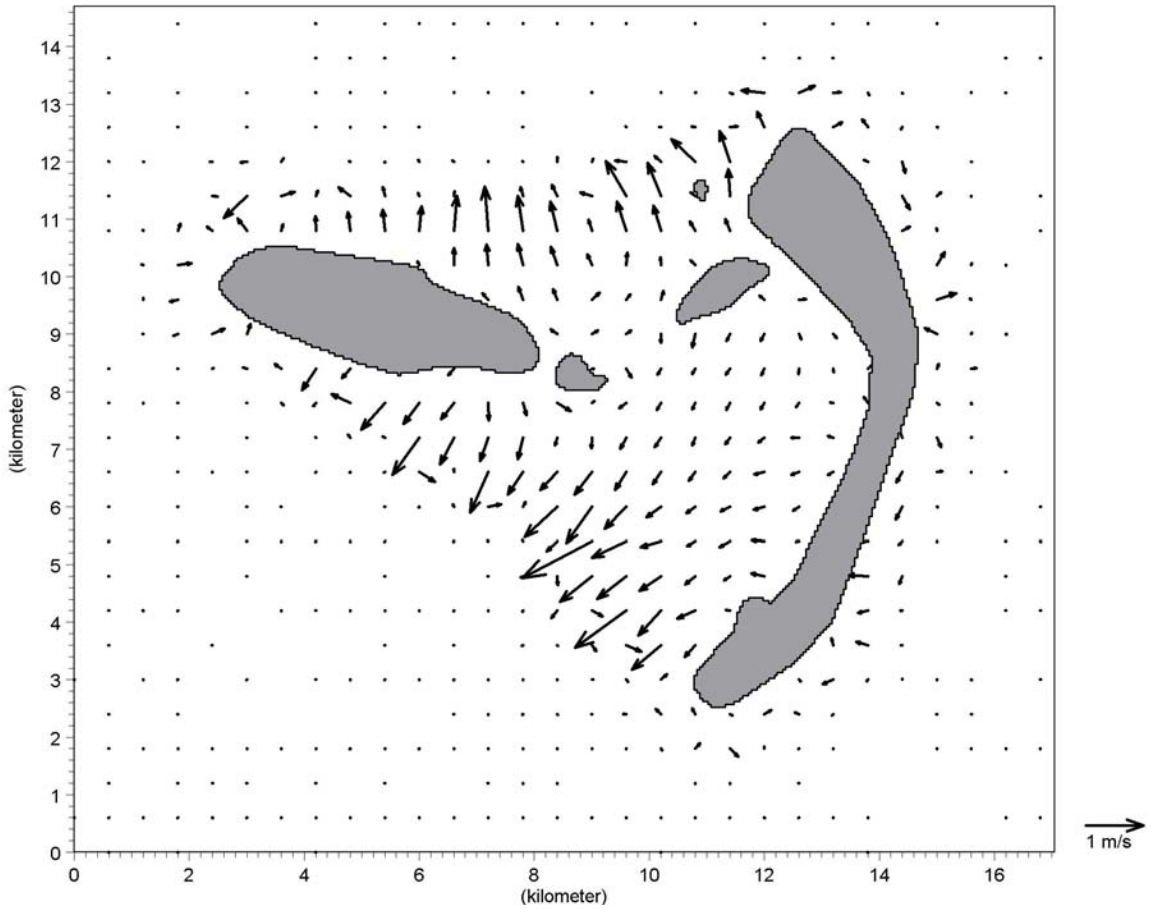


MIKE21 tide simulation with 2.5 m amplitude tides. Image generated during ebb stage of tidal cycle. True north is at the top of the image.

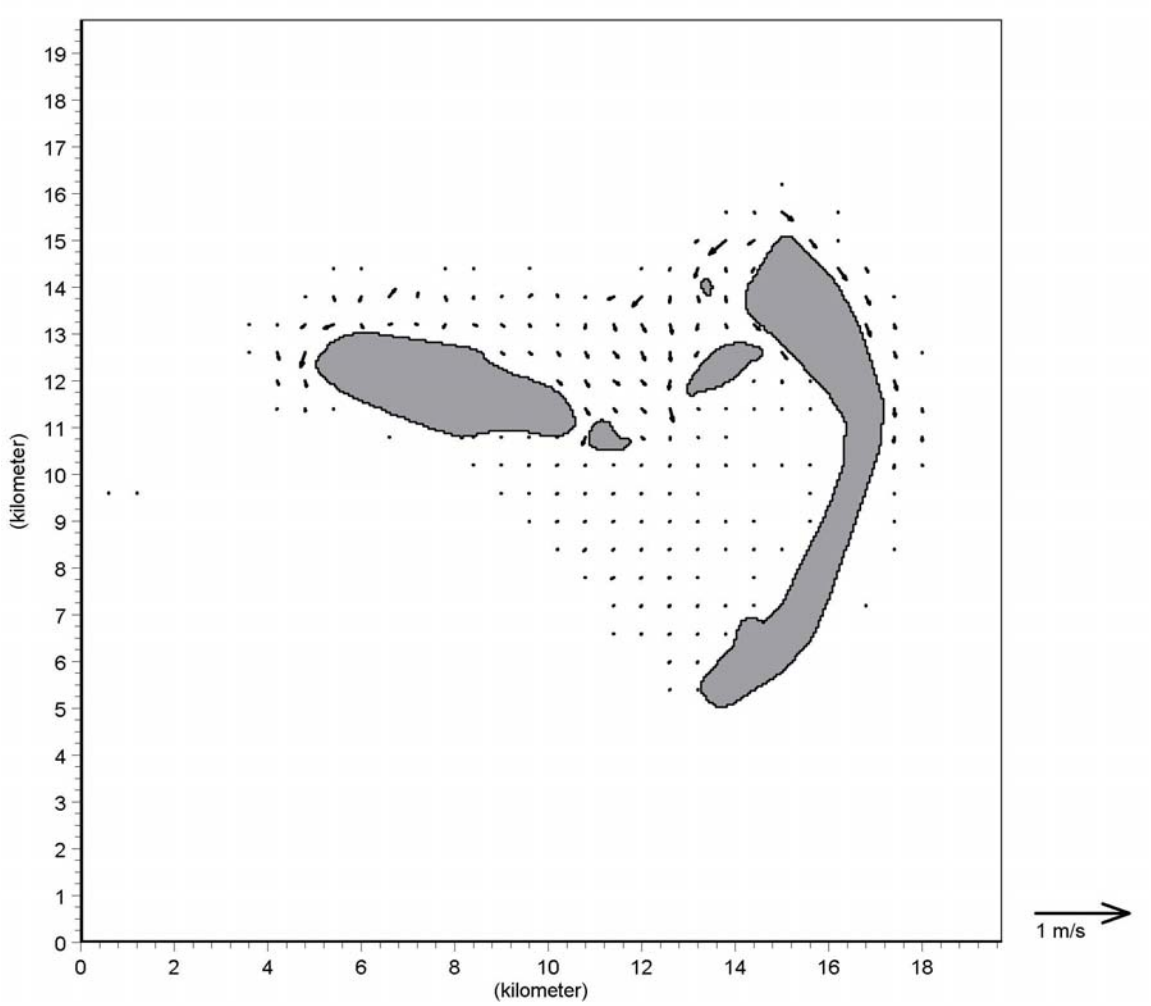


MIKE21 wave simulation with waves generated from the north (0°) with a 2 m wave height. True north is at the top of the image.

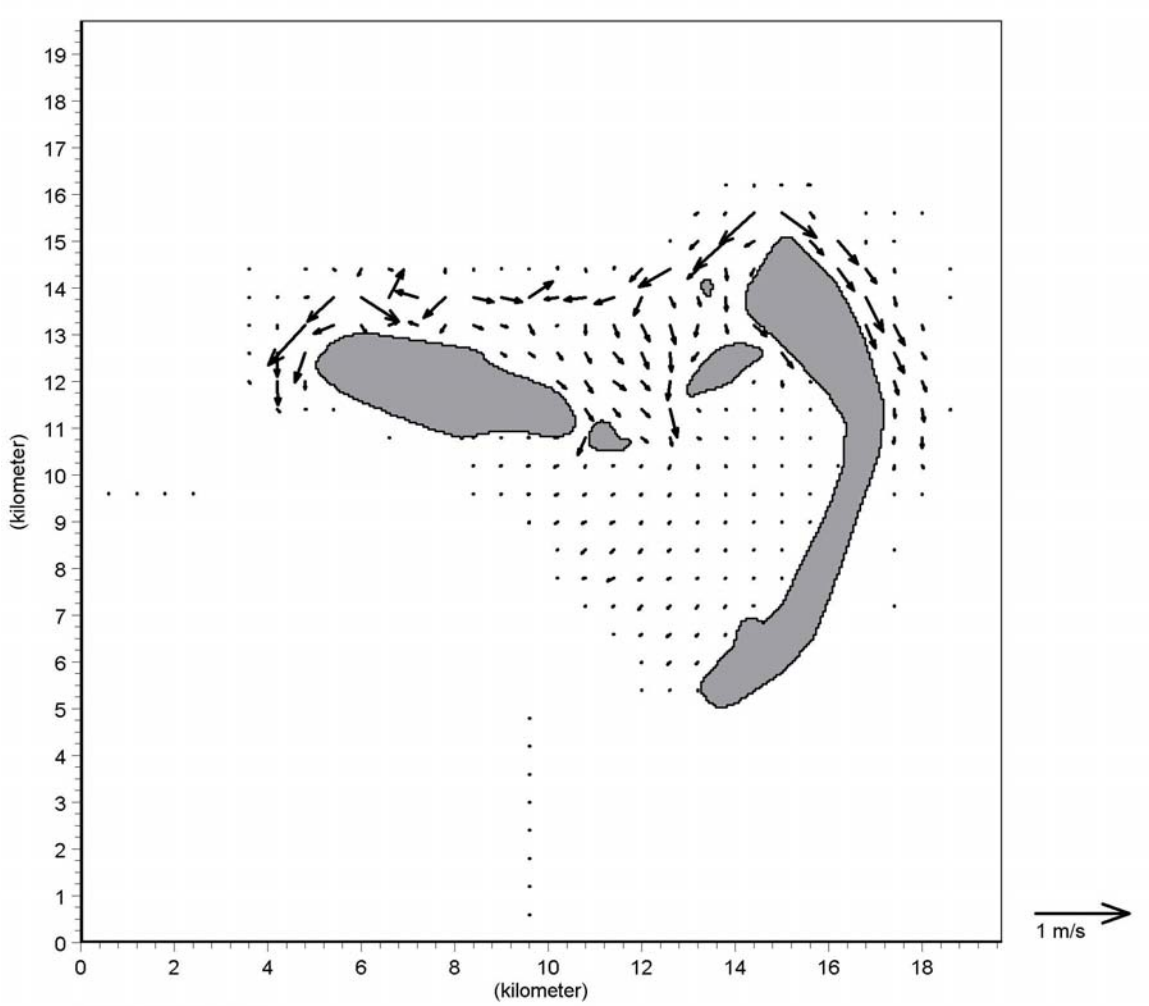


MIKE21 wave simulation with waves generated from the north (0°) with a 4 m wave height. True north is at the top of the image.